CHAPTER 5 COAL PILLAR

5.1 INTRODUCTION

A **coal pillar** is a block of coal left in its natural state to support the weight of overburden and to protect the integrity of the entries and crosscuts adjacent to it, thereby allowing miners to extract coal between them and to travel safely. Coal pillars are the foundation of, and thus a very important structure in, U.S. underground coal mines.

5.1.1 Types of Pillars

1. By Objective

By its objective, coal pillars can be divided into two types: chain pillars and barrier pillars. **Chain pillars** are those rows of pillars aligned in the mains, submains, production panels or sections, and longwall gateroads and bleeder systems. A **barrier pillar** is a solid coal block designed to isolate the effect of mining on one side of the block from the other side. Chain pillars are shorter and smaller, normally square or rectangular or sometimes parallelepiped in shape, while a barrier pillar is wider and much longer in comparison to its width. Consequently, there are many more chain pillars than barrier pillars (see Fig. 1.3.1, p. 4) in an underground coal mine.

An **outcrop barrier pillar** is that block of coal left around the outcrop perimeter of an above-drainage mine. It is designed to avoid accidentally punching out into the atmosphere and to prevent the impounded water, after mine abandonment, from blowing out.

Web pillars are the small pillars left between adjacent cuts in highwall mining. Their length is extremely long, up to 1,500 ft (457.3 m), as compared to their width.

2. By Mechanism

By its mechanism, coal pillars can also be divided into two types: stiff (abutment) pillars and yield pillars. **Stiff pillars** are designed to support the expected load that the pillars will experience throughout their service life, while a **yield pillar** is designed to yield at the proper time and rate, and in so doing transfer a proper amount of load to adjacent supporting blocks of coal. In other words, a yield pillar is not designed to take the load during any stage of its service life.

Stiff pillars are predominantly used in U.S. underground coal mines. Yield pillars are used exclusively in deep mines where the required stiff pillars are too large to be economically viable, or where geological and mining conditions are prone to bumps and/or floor heaves.

5.1.2 Procedures of Pillar Design

The procedure and method of stiff pillar design are completely different from those for yield pillars, due to difference in supporting mechanisms and objectives. Since stiff pillars have been predominantly used from the inception of coal mining and nearly all pillar design methods are for stiff pillars, the procedure and method of pillar design described in this book, unless otherwise specified, are for stiff pillars. Consequently, the terminology “pillar” refers simply to a stiff pillar.

The procedure and method of yield pillar design is discussed in Section 5.4.2, p.260. There are three major steps in pillar design: (1) determination of expected load on the pillar throughout its service life, (2) determination of pillar strength, and (3) determination of the

factor of safety. These three steps seem to be simple, but uncertainties and thus controversies are abundant in every step.

1. Load on Coal Pillar

Depending on the mining method employed, a coal pillar during its service life is first subjected to a development load during entry/crosscut development and then abutment load if pillar extraction or longwall mining is employed.

In recent years, all researchers and practitioners generally agree that the applied (development) load on a chain pillar during development of entries/crosscuts can be calculated by the tributary loading concept, i.e., the load is equivalent to the weight of the overburden rock block, consisting of its cross-sectional area plus the area along half the width of the openings surrounding its four sides. This approach assumes that this block of overburden is separated completely from the adjoining overburden with its weight totally resting on the pillar below. This, in most instances, tends to over-estimate the pillar load. Because computer analysis shows that, depending on the characteristics of the overburden strata, this method of load calculation can either over- or under-estimate the apply load on a pillar, depending on the stratigraphic sequence of the overburden. For example, Hill et al., (2008) found that in Australia's NSW Southern coalfield, main headings pillar widths are commonly 49.2 – 82 ft (15 – 25 m) wide at depths of 984 – 1,640 ft (300 – 500 m). If the tributary loading is applicable, those pillars would have failed.

Based on the tributary loading concept, the development load on a pillar can be calculated by

$$\sigma_a = \frac{(W_p + W_o)(L_p + W_o)}{W_p L_p}\sigma_v \tag{5.1.1}$$

where σ_a is development stress (psi), W_p, L_p, and W_o are pillar width, pillar length, and entry/crosscut width, respectively, $\sigma_v = 1.1h$ (psi) is vertical stress due to overburden rock weight, and h is depth of cover (ft).

Equation 5.1.1 can be expressed in terms of coal extraction ratio as

$$\sigma_a = \frac{1.1\,h}{1 - R} = \frac{1.1\,h}{1 - \dfrac{W_o}{W_p + W_o}} \tag{5.1.2}$$

where R is extraction ratio.

2. Strength of Coal Pillars

There are many pillar strength formula developed for various coal fields in the world (Babcock et al., 1981; Bieniawski, 1981; Hustrulid, 1976; Iannacchione et al, 1992; Mark et al., 1999; VPI&SU, 1981). A general agreement among researchers is that the strength of a coal pillar increases with the pillar's width-to height ratio, following two general types of equations: linear and power,

$$S_p = S_{cube}\frac{W^{\alpha}}{H^{\beta}} \tag{5.1.3}$$

$$S_p = S_{cube}(A + B\frac{W}{H}) \tag{5.1.4}$$

where S_p is pillar strength with width W and height H, S_{cube} is the strength of a cubical pillar, and α, β, A, and B are constants.

The major problem with these formulae is that constants α, β, A, and B are different for different strength formulae, resulting in different pillar strengths. Consequently, adoption of any one of the strength formulae for a design application will produce different design results, even though some formulae show only minor differences.

Furthermore, the strength of a cubical pillar, S_{cube}, in Equations 5.1.3 and 5.1.4 is normally derived from laboratory-sized coal specimens. The strength of laboratory-sized cubical specimens, ranging from 1 in. to 6 in. (25.4-152.4 mm), is known to decrease with increasing specimen dimension. However, due to the large variation of strength obtained for each size of specimen, the relationship of strength reduction between specimen size and coal strength is not totally unique, although it can usually be represented by an exponentially decaying curve.

3. Factor of Safety

The **factor of safety** is defined as the ratio of pillar strength to pillar loading, or for cases involving development load only,

$$SF = \frac{S_p}{\sigma_a} \tag{5.1.5}$$

In engineering, the factor of safety is used to account for uncertainty. It is most appropriate for the design of underground coal pillars, because the prevailing methods for determining both pillar loading and pillar strength involves a high degree of uncertainty. The higher the factor of safety, the lower the probability of failure. The factor of safety recommended for various pillar design formulae varies from 1.3 to 5 (Holland, 1973).

Table 5.1.1 shows the relationship between the factor of safety and probability of failure (Bieniawski et al., 1994; Hoek, 1993; Galvin et al., 1999). The coefficient of variation is a statistical measure of the dispersion of data points in a data series around the mean. It is defined as the ratio of standard deviation to the mean. The larger the coefficient of variation, the larger the spread of data points in a test. When the factor of safety is one, there is 50 % probability of failure, regardless of the coefficient of data variation. When the factor of safety is 1.5, the probability of failure varies from zero to 14 in 100 when the coefficient of variation ranges from 0.05 to 0.25.

Due to the large standard deviation of data points in every batch of laboratory test coal specimens for uniaxial compressive strength, the coefficient of variation is very large, and subsequently, the factor of safety must be larger in order to reduce the probability of failure. When a large factor of safety is chosen, the result may be unnecessarily over-designed. The most effective way that has been universally adopted in all ground control research and design is to calibrate the proposed coal pillar strength with surveyed data of failure and success cases in coal mines and determine the proper factor of safety. The greater number and better quality of case studies collected, the higher the confidence level for the proposed formula. With this approach, nearly all proposed formulae can be used for pillar design, once calibration with case studies is done and a proper factor of safety is determined.

Table 5.1.1 Probability of failure (%) for different combination of factor of safety and coefficient of variation (Bieniawski, 1994; Hoek, 1993)

Coefficient of variation	Factor of safety						
	1.00	1.25	1.50	1.75	2.00	2.25	2.50
0.05	50.0	0.1	0.0	0.0	0.0	0.0	0.0
0.10	50.0	6.7	0.3	0.0	0.0	0.0	0.0
0.15	50.0	15.9	3.6	0.8	0.2	0.0	0.0
0.20	50.0	22.7	8.8	3.4	1.4	0.6	0.3
0.25	50.0	27.5	14.0	7.2	3.9	2.3	1.4

5.2 FACTORS AFFECTING PILLAR STRENGTH

In addition to the geometrical factors stated in the previous section, the rock mechanic properties of materials forming the coal pillar and the non-uniform stress distribution induced within a coal pillar also greatly influence pillar strength.

Coal is a geological material. As such, the single most important factor affecting its strength is its components and their occurrence. Underground coal pillars are complex heterogeneous materials, consisting of different macerals, partings, cleats, beddings planes, and joints/fractures, each of which contributes in different degrees to the strength of the coal pillar.

According to Babcock (1985), constraint on the top and bottom ends of specimens is the prime variable in pillar strength. In this respect, there are four factors that contribute to pillar strength: First, when the angle of internal friction changes from 30^o to 60^o, pillar strength increase by a factor of two. Second, if the roof and floor rocks are strong, a given pillar will become stronger. Conversely, the pillar becomes weaker. Third, the apparent increase in pillar strength is related to pillar width, not pillar height. This factor can easily change the apparent strength by a factor of five. Fourth, the effect of end constraint can make a larger pillar either stronger or weaker. This factor can also change pillar strength by a factor of five.

5.2.1 Geometry of Pillars

The geometry of pillar refers mainly to the size of the cubical pillar and slenderness of a prismatic pillar. The effects of these two parameters on rock and coal strengths have been known since 1876.

It is an established fact that the strength of laboratory-size coal specimen decreases exponentially with increase in size (Fig. 5.2.1) until the specimen reaches a certain threshold size above which the strength approaches a constant value. This effect is commonly attributed to the fact that the larger the specimen the more defects it contains and thus the lower the strength.

The fact that the strength of a laboratory-size specimen increases with an increase in its width-to-height ratio was found as early as 1876 by Bauschinger (as described by Johnson in

1897 and Bunting in 1911) when he tested Swiss sandstone and developed the following linear equation that has been cited often by contemporary researchers

$$S_p = S_{cube}(0.778 + 0.222\frac{W}{H}) \tag{5.2.1}$$

where S_p and S_{cube} are strength of prism and cube, respectively, and W and H are the width and height of the specimen, respectively. Note that Equation 5.2.1 has been wrongfully referred to as the Obert and Duvall formula in all of the previous publications. This formula will be correctly referred to as the Bauschinger formula in this book.

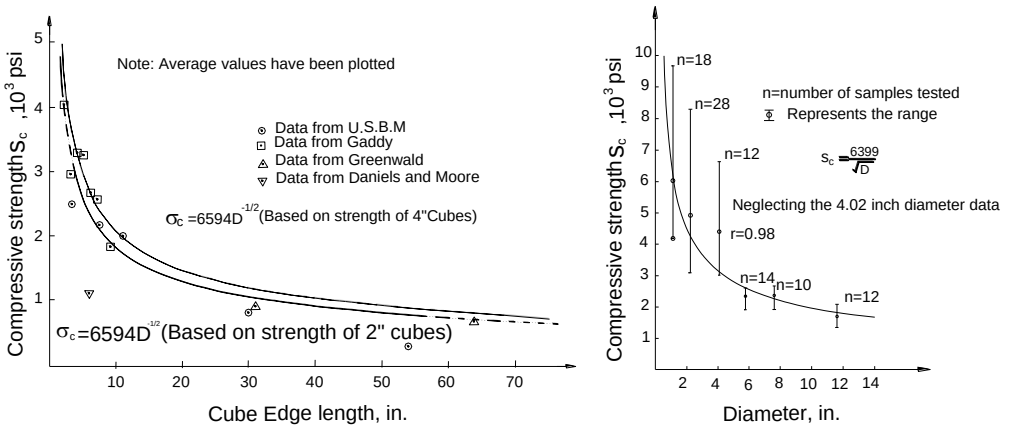

Fig. 5.2.1 Compressive strength of coal as a function of specimen size: A, cubical specimens, and B, cylindrical specimens (Pariseau et al., 1977)

In testing cubical coal specimens ranging from 2 to 6 in. (50.8-152.4 mm), the crushing strength of small cubes was found to be greater than that for larger cubes by Daniels and Moore (1907). They also confirmed that with a constant base area, increasing specimen height, the crushing strength becomes smaller.

In a comprehensive testing program on the compressive strength of anthracite coal, a total of 425 samples of 2 x 2 x 1 in. (50.8 x 50.8 x 25.4 mm), 2 x 2 x 2 in. (50.8 x 50.8 x 50.8 mm), and 2 x 2 x 4 in. (50.8 x 50.8 x 101.6 mm) were tested and the results published by Griffith and Conner (1912). The squeezing strength required to produce the first crack in the sample with width-to-height ratio equal to 2 was 3,000 psi (20.7 MPa), and the crushing strength required to crush the samples was 6,000 psi (41.4 MPa). And in general, everything being equal, the crushing strength of mine pillars would vary inversely as the square root of the pillar height and increase with sample width-to-height ratio.

In determining the strength of West Virginia coals, Lawall and Holland (1937) prepared and tested 223 samples of 3 in. (76.2 mm) cubes from 33 coal seams. They found that coal strength varies from 1,163 to 6,861 psi (8 to 47.3 MPa); that the UCS of coal is less when determined on large cubes than when determined on small cubes; and that the coals have very good weathering properties.

The results of these studies on the effects of pillar size and shape on pillar strength form the fundamental basis of all modern coal pillar strength formulae.

5.2.2 Constitutive Materials of Coal Pillars

Coal is composed of three major distinct organic groups called **macerals**, vitrinite, liptinite, and inertinite. Very often each group forms a separate layer in a coal seam. Vitrinite is the most abundant group and is derived from the woody tissue of plants. It looks dull. Inertinite has a charcoal like structure. It is brittle and appears bright. Liptinite is derived from waxy and resinous parts of plants. It is resistant to weathering. Both liptinite and inertinite are more abundant in Appalachian coals.

Therefore, every coal seam is composed of several bands of anisotropic and non-homogeneous materials, the material properties of which differ. Consequently, due to the difference in structure, the UCS of samples may be quite different, depending on the position of the sample, with respect to the height of the seam and the working face in the mine. For instance, Fig. 5.2.2 shows the average uniaxial compressive strength of various bands obtained from Warfield and Coalburg seams (Unrug et al., 1987). The UCSs of various bands vary from 1,369 to 5,639 psi (9.44 to 38.88 MPa) and from 1,075 to 6,077 psi (7.41 to 41.90 MPa) for Warfield and Coalburg seams, respectively. Obviously, the weak layers, especially the weakest and thickest ones, will control the deformation, and ultimately, the strength of a coal pillar. With such a wide variation of UCS at different levels of the coal seam, **seam strength**, rather than **coal strength of a coal pillar,** is more appropriate.

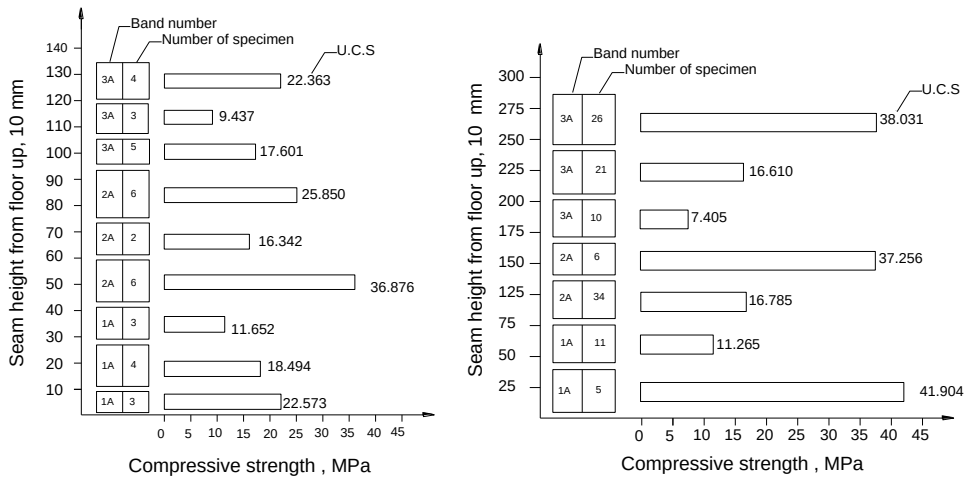

A. Warfield Seam **B. Coalburg seam**

Fig. 5.2.2 Variation of UCS with various bands in coal seams (Unrug et al., 1987)

Coal seams always contain one or more layers of partings at different elevations. Those partings are normally weaker and more susceptible to weathering than coal material. But sometimes they may be stronger or about the same as the host coal. They may be uniformly distributed, but most often they vary in thickness from place to place, sometimes even within a pillar (Unrug and Turner, 2005). It is the thickness and strength of the weakest layer within the seam that governs the extent to which the pillar would be able to perform satisfactorily, because a thicker low-strength layer would deform more than any other layers, thereby initiating the process of shortening and extrusion of the pillar (Unrug, et al., 1987; Esterhuizen and Ellenberger, 2007; Esterhuizen et al., 2006).

The effect of rock partings in coal on pillar strength depends on the parting strength. A weak parting rock, such as claystone, can fail prematurely, thus increasing the depth of yielding of the pillar, thereby reducing the peak pillar strength. Conversely, a stronger rock, such as shale parting, effectively reduces pillar height, thereby increasing the width-to-height ratio and, subsequently, the peak pillar strength. (Fig. 5.2.3) (Su and Hasenfus, 1997). For a strong parting, the pillar strength gradually approaches that for pillars without partings with increasing width-to-height ratio.

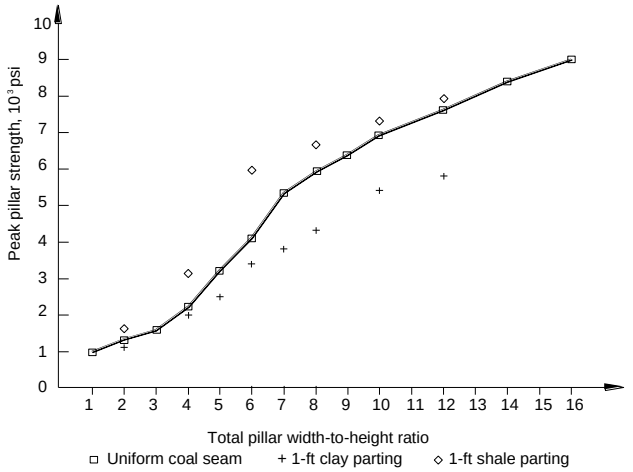

Fig. 5.2.3 Effect of seam strength on the ultimate strength of coal pillars (Su and Hasenfus, 1997)

Coal is an orthotropic material because it contains three mutually perpendicular planes of weaknesses, i.e., bedding planes, face, and butt cleats. Therefore the elastic properties, and consequently their behavior, are different in the directions perpendicular to these three mutually perpendicular planes.

5.2.3 Effects of Coal/Roof and Coal/Floor Interfaces

As stated in Section 2.6.1 on p. 53, due to difference in elastic property, a frictional force developed at the interface between the coal seam top and immediate roof and between coal seam bottom and immediate floor. Friction can be positive or negative. With positive friction, the seam top or seam bottom area is restricted or confined to expand laterally, resulting in a triaxial state of stress and increasing coal strength. Whereas, with negative friction, the material near the coal seam top or bottom area is pulled apart, resulting in an extension state of stress and decreasing coal strength. Therefore, coal seam or pillar strength is a function of the property of coal top/roof and coal bottom/floor interfaces.

Researchers unanimously agree that the existence of a confined core in a pillar accounts for the fact that pillar strength increases with increasing pillar width-to-height ratio and that confinement under strong immediate roof and floor increases. The triaxially-stressed or confined core area at the center of a pillar increases with increasing pillar width-to-height ratio. However, the width-to-height ratio below which a pillar has no or little confinement, and above which the size of confined core increases with the width-to-height ratio varies from 3 to 7 or 8 according to different researchers (Galvin et al., 1999; Holland, 1858b; Mark and Chase, 1997; Stacy and Page, 1986). Therefore, it is probable that when the width-to-height ratio is

less than 3, pillar strength depends more on the inherent coal properties rather than the surrounding rock strata.

Conversely, when negative friction exists on the coal top/roof or coal bottom/floor interface, there is no confined core within the pillar, and the coal pillar will fail by vertical rib spalling due to horizontal tensile force or buckling of a thin column. A negative friction force will be generated when the immediate roof or floor is weak and prone to flow laterally upon loading (Greenwald, et al., 1939; Gale, 1998 and 1999), resulting in lower pillar strength.

Numerical modeling by Su and Hasenfus (1997) showed that compared to a strong floor (Fig. 5.2.4), a weak claystone floor may significantly reduce the ultimate peak pillar strength as a result of reduced pillar confinement near the floor interface; that the difference in peak pillar strength increases with increasing pillar width-to-height ratios; and that beyond the width-to-height ratio of 8, the peak strength asymptotes toward a maximum value. At high width-to-height ratio, the peak strength reduction is nearly 50%.

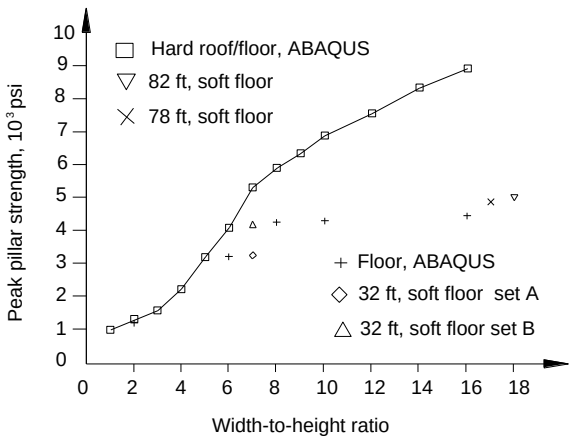

Fig. 5.2.4 Effect of weak claystone floor on the ultimate strength of coal pillars (Su and Hasenfus, 1997)

Therefore, the property of the interface between pillar top and immediate roof and between pillar bottom and immediate floor is a major factor that cannot be ignored in pillar design. In this respect, it is reasonable to state that all laboratory-determined rock strengths are not intrinsic. Rather, they are the product of interface properties between machine platen and specimen top and bottom.

Numerical analysis shows that confinement, expressed by the magnitude and area of the minimum principal stress generated in the pillar, increases with increasing width-to-height ratio and shear strength of the coal/rock interface (Lu et al., 2008). However, the effect of interface shear strength is much more significant than the width-to-height ratio. Confinement is low when the interface is weak even with a high width-to-height ratio. Conversely, confinement is high when the interface shear strength is strong (Fig. 5.2.5). Confinement is also responsible for the post-failure behavior of the pillar, i.e., strain softening or strain hardening. The transition from strain softening to strain hardening behavior depends on a proper combination of pillar width-to-height ratio and interface shear strength. Fig. 5.2.6 shows that when interface shear strength is low, the pillar exhibits strain softening behavior regardless of the width-to-height ratio. As the interface shear strength increases, the transition from strain softening to strain hardening behavior occurs at a lower width-to-height ratio.

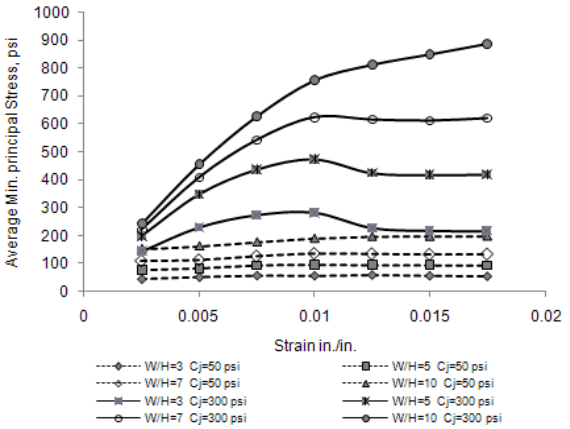

Fig. 5.2.5 Average minimum principal stress with different with-to-height ratio and interface shear strength (Lu et al, 2008)

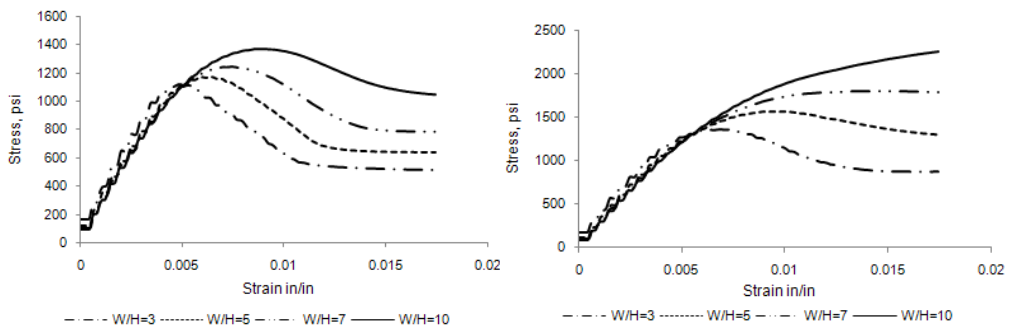

A. Interface shear strength 50 psi **B. Interface shear strength 150 psi**

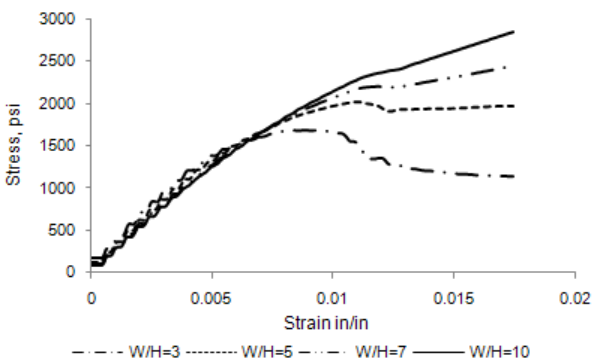

C. Interface shear strength 300 psi

Fig. 5.2.6 Stress-strain curves of pillar under different width-to-height ratios and interface shear strength (Lu et al., 2008)

Figure 5.2.7 demonstrates a practical example of importance when considering the immediate roof and floor strata in pillar behavior (Peng, 2007; Peng and Dutta, 1992).

A **B**

Fig. 5.2.7 A, trial section of pillar design and B, floor heave in the 50 x 50 ft (15 x 15 m) pillar area (Peng, 2007; Peng and Dutta, 1992)

The coal seam was 6 ft (1.8 m) thick under 875-912 ft (266.7-278 m) cover. In order to determine a proper pillar size for the mine, a test section 600 ft (182.8 m) wide by 1,000 ft (304.8 m) long was developed in which three sizes of chain pillars, i.e., 70 x 80 ft (21.3 x 24.4 m), 50 x 50 ft (15.2 x 15.2 m), and 60 x 60 ft (18.3 x 18.3 m) center to center were used. The entries and crosscuts were 18 ft (5.5 m) wide (Fig. 5.3.2A). The immediate roof was gray or sandy shale with UCS 11,500 psi (79.3 MPa), and the immediate floor was fireclay with UCS (dry) 5,722 psi (39.5 MPa). In the areas with 70 x 80 ft (21.3 x 24.4 m) and 60 x 60 ft (18.3 x 18.3 m) centers, the pillars remained intact and stable throughout the mine life. But the area with 50 x 50 ft (15.2 x 15.2 m) centers pillars deteriorated rapidly soon after development. Degradation began with sudden buckling of the immediate floor in the entry and crosscut centers and hove up 2-3 ft (0.61-0.91 m), followed by rib spalling up to 4-5 ft (1.2-1.5 m) deep. In this case, all three pillar sizes were sufficiently strong to support the roof, but the 50 x 50 ft (15.2 x 15.2 m) centers pillars were too small for the fireclay when wet and could not be used for production operations.

5.2.4 Fractures in Coal Pillars

Fractures in coal include faults, joints, and cleats. Pillar strength is lowest when the fractures are oriented approximately 30-40^{o}, and largest when they are oriented perpendicularly, to the vertical axis of the pillar (see Fig. 2.6.12, p. 62) (Esterhuizen et al., 2006; Iannacchione, 1999).

Laboratory tests of coal samples from two different coal seams in Illinois showed that the factors that affected the strength of coal samples are number of discontinuities, angle of critical discontinuities, and shape of sample. Among them the most important factor is the angle of critical discontinuities (Kroeger et al., 2004) which is about 60^{o} from the loading axis.

Cleats include face and butt cleats. They are vertical and mutually perpendicular to each other. Depending on the orientation of entry and crosscut with respect to those of the cleats, cleats may facilitate rib spalling and pillar corner rounding (see Section 3.3.1 on p. 94).

Figure 5.2.8 shows an example of pillar failure due to fault and joints.

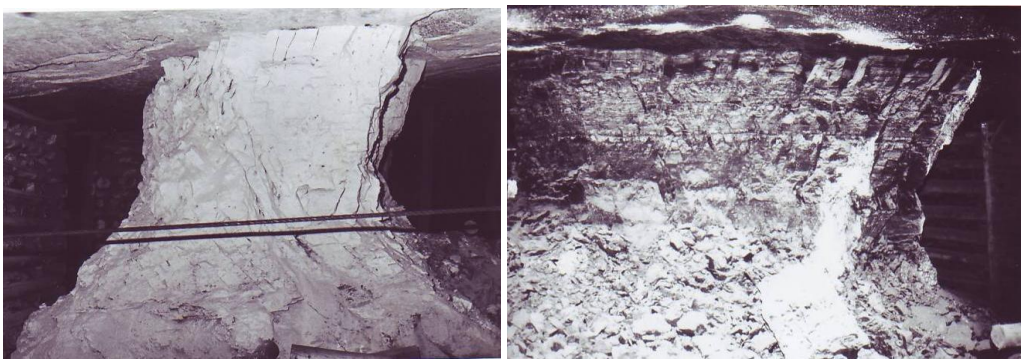

Fig. 5.2.8 Failure of pillars due to fault (left) and joints (right) (Mokgokong and Peng, 1991)

5.2.5 Panel Dimension

Panel dimension refers to the size of the area of mining. As the development of entries and crosscuts continues, the area of development continues to expand. Although many pillars were stable initially, when the development area reaches critical dimensions, depending on the characteristics of the overlying and underlying strata and pillar size and layout pattern, massive pillar collapse may occur. This problem was recognized far back in 1911 by Bunting who said "To mine without leaving adequate pillar supports will result, sooner or later, in a squeeze. limited areas, it is true, have been mined at certain widths of chambers and pillars, without caving or squeezing; but this is not positive proof that such pillars would be of sufficient size, under the same conditions of thickness of vein and depths below the surface, for larger areas; for frequently a squeeze will not be induced until a large area has been mined." **Squeeze** is crushing of pillars, followed by a breaking and caving of the roof, and heaving or lowering of the floor.

Many cases of massive pillar failures over the last three decades have been documented (Peng, 2007). In all cases, the individual pillars in the areas of massive pillar failures were stable and functioned normally. They failed when the area of mining continued to expand contiguously until it reached critical dimensions. An example of massive pillar failure is shown in Fig. 5.2.9. The coal seam was 62 in. (1.6 m) thick and 400 ft. (122 m) deep, at a, decreasing to 220 ft. (67.1 m) deep at b. Chain pillars were developed at 60 x 60 ft (18.3 x 18.3 m) center-to-center with an entry and crosscut width of 20 ft (6.1 m). Retreat mining began at the point a side and advanced toward point b side. During retreat, each pillar was split by making a center cut, 20 ft. (6.1 m) wide (hatched area in Fig. 5.2.9A) on the entry direction, leaving a remnant pillar of 10 x 40 ft. (3.1 x 12.2 m) on each side. The remnant pillars remained stable up to the point when retreat mining had advanced and covered areas A and B. Two days after Area B was completely retreated, pillar failure was initiated at point b and propagated to cover areas A and B in eight hours. Figure 5.2.9B is the cross sectional view at 2.

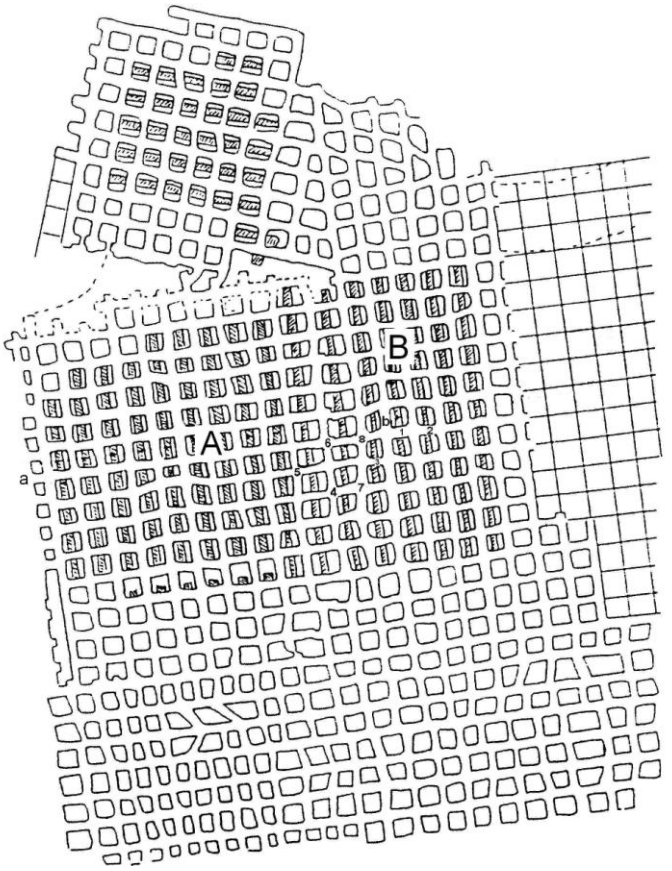

A. Section layout

B. Cross sectional view of pillar failure

Fig. 5.2.9 An example of massive pillar failure (Peng, 2007)

5.3 PILLAR DESIGN METHODS

Based on the evolution of a pillar design concept, pillar design can be divided into three categories in order of increasing sophistication and complexity: (1) the conventional formula

for individual pillar method, (2) semi-conventional method for a group of pillars, and (3) mine structural analysis. This type of classification is designed to illustrate the importance of treating coal pillars as a structural element of the overall mine structure, not as a stand alone unit.

5.3.1 Conventional Formulae for Individual Pillars

1. Pillar Strength Formula

The conventional pillar design formulae are designed for an individual pillar independent of all other pillars surrounding it. It also assumes that the pillar is composed of homogeneous and isotropic materials, and that upon loading, the vertical stress within the pillar is uniformly distributed.

The first U.S. coal pillar design formula was developed by Bunting (1911) for deep anthracite mines. He used the data collected by Griffith and Conner (1912) and developed the following formula:

$$S_p = 700 + 300\frac{W}{H} \tag{5.3.1}$$

where S_p is the strength of the pillar, the width and height of which are W and H, respectively. The strength of 1 in. (25.4 mm) cubical specimens was 2,500 psi (17.2 MPa). When he attempted to fit Equation 5.3.1 to 6 cases of underground coal pillar squeezes, he found the pillar strength could be represented by,

$$S_p = 1000(0.70 + 0.30\frac{W}{H}) \tag{5.3.2}$$

where he defined the cubical pillar strength as S_{cube} = 1,000 psi (6.9 MPa). Since the compressive strength of the 1 in. (25.4 mm) cubical specimen was 2,500 psi (17.2 MPa), a strength reduction factor or a safety factor of 2.5 was used, and the generic form of the pillar strength formula became,

$$S_p = S_{cube}(0.70 + 0.30\frac{W}{H}) \tag{5.3.3}$$

The next pillar design formula was developed by Greenwald et al., (1939) and Greenwald (1941) who performed five in-situ coal pillar strength tests for the Pittsburgh seam with pillar dimensions ranging from 3.15 ft to 6.3 ft (0.96 to 1.92 m) in side dimension. The strength of pillars ranged from 700 to 930 psi (4.8 to 6.4 MPa) and can be presented by (Holland, 1964)

$$S_p = 2{,}800\frac{W}{\sqrt[6]{H^5}} \tag{5.3.4}$$

$$S_p = 900\sqrt{\frac{W}{H}} \qquad \text{(for W/H < 1)} \tag{5.3.5}$$

Holland (1942) found that when W/H is small, specimens fail abruptly. As W/H increases a point will eventually be reached such that the specimen does not fail abruptly, but rather is forced to squeeze. For weaker coals, this point is W/H = 5 and for strong coals, it is W/H = 7 (see Table 9.3.1 on p. 438). Extrapolation of this laboratory data gave a result that implies that when W/H is greater than 10-12, pillars develop extremely high compressive strength.

Considering the variability of coal, Gaddy (1956) found the following relationship between the strength of a cubical specimen and its absolute size as,

$$S_p = \frac{K}{\sqrt{D}} \tag{5.3.6}$$

where S_p is the strength of a cubical coal specimen having edge dimensions of D. K is a coefficient depending on the characteristic of the coal tested.

Based on the historical experimental data, Holland and Gaddy (1957) proposed the following formula, which is known as the Holland-Gaddy formula,

$$S_p = K\frac{\sqrt{W}}{H} \tag{5.3.7}$$

where S_p is the mean strength of the coal pillars (psi), W is the least width of the pillars (in.), H is the height of the pillars (in.), and K is a coefficient depending on the characteristic of the coal tested (lbs/in$^{3/2}$). The value of K for any coal seam can be obtained by testing the UCS of a sufficient number of cubical specimens for the coal seam under consideration. The size of the cube should be between 2 and 4 in. (50.8 and 101.6 mm). To be representative of the coal seam, such as in a 5 ft seam, no less than 30 cubes should be tested. Over 5 ft thick, add 6 cubes per foot of thickness. Samples should be taken from 10 to 15 locations over the area to be mined (Holland, 1973). The Holland-Gaddy formula is not valid when W/H is less than 1 and greater than 12. The recommended factor of safety is 1.7-2.0. Holland (1973) also recommended that after the size of the pillar is determined, it should be checked against the bearing capacity of the floor for potential pillar punching into the floor. The bearing capacity of the floor can be assumed to be equal to its uniaxial compressive strength.

Through a study of measurements of pillar strength and deformation in situ and laboratory compression tests of small specimens, Skelly et al., (1977) found that it is feasible to predict the strength of coal mine pillars by applying laboratory core test data and that their experimental data supported Equation 5.2.1. In the underground test, a pillar was systematically trimmed off on three sides until it failed.

After the Coalbrook disaster in 1960 in which more than a thousand pillars collapsed and 437 miners were killed (van der Merwe, 2006), South Africa began to research pillar design with two approaches: in-situ pillar strength tests and back analysis of cases of pillar failures. Backed by the coal industry, Salamon and Munro (1967) analyzed 27 cases of pillar failures and 92 intact pillars, and developed the following pillar strength formula,

$$S_p = 7.716\frac{W^{0.46}}{H^{0.66}} \tag{5.3.8}$$

Note that Equation 5.3.8 uses SI units.

Later, Salamon (1982) found that, contrary to experimental trends, Equation 5.3.8 predicts the decreasing rate of strength increase as W/H increases. He then extended the strength formula for wide (or squat) pillars as

$$S_p = k\frac{R_0^b}{V^a}\left\{\frac{b}{\varepsilon}\left[\left(\frac{R}{R_0}\right)^{\varepsilon} - 1\right] + 1\right\} \tag{5.3.9}$$

where V is pillar volume, R_0 is the critical width-to-height ratio at which the formula becomes valid, $\mathcal{E}$ is the rate of strength increase, and a and b are material constants. According to Madden (1991), R_0 = 5, $\mathcal{E}$ = 2.5, a = 0.0667, and b = 0.5933. The recommended safety factor for panel mining is 1.6 and for main development is 2.0 (Salamon and Oravecz, 1976). However, after examining the new data that included pillar failures at high safety factors within a short period of time after their creation, Van der Merwe (2002) found that the separation between the population of failed and stable pillar cases can be improved by 22 % by adopting the following linear formulae for South African coals

$$S_p = 3.5\frac{W}{H} \qquad \text{for "normal" coal} \tag{5.3.10}$$

$$S_p = 1.5\frac{W}{H} \qquad \text{for "weak" coal} \tag{5.3.11}$$

Based on a series of 57 underground in-situ coal pillar strength tests (Bieniaswki, 1968a and 1968b; Bieniawski and van Heerden, 1975; Wagner, 1974) in South Africa, Bieniawski (1983) found that the following pillar strength formula is applicable to any coal seam, provided the value of S_{cube} is known,

$$S_p = S_{cube}(0.64+0.36\frac{W}{H})) \tag{5.3.12}$$

where S_{cube} is the strength of a critical size of cubical pillars. The **critical size** is 3 ft (0.9 m) is that above which pillar strength no longer decreases with increasing size of pillar, i.e., above which pillar strength remains more or less a constant. For the Pittsburgh seam, S_{cube} is estimated to be 930 psi (6.4 MPa) (Bieniawski, 1992).

It is interesting to note the similarity between Equations 5.3.3 and 5.3.12. The former was derived from laboratory-sized anthracite specimens, while the latter was from in-situ bituminous coal pillar tests.

Bieniawski (1983, 1992) performed a survey of U.S. coal mines in 1982 and obtained a total of 174 cases of pillar stability for analysis, including 23 cases of pillar failures. By calibrating with this set of data as shown in Fig. 5.3.1, he concluded that for room-and-pillar mining, the recommended factor of safety is 1.5-2.0 and for longwall mining, it is 1.3.

As case studies accumulated, Mark (1999) revised the recommended safety factor for the Bieniawski square pillar formula to

$$SF = 1.76 - 0.014\ CMRR$$

where *CMRR* is coal mine roof rating.

2. Pillar Design Procedure

In recent years, it is generally agreed that the determination of underground pillar strength using the conventional design formula method involves three sequential steps: Step 1, determination of underground cubical pillar strength-size effect. A **critical underground cubical pillar** is defined as that with side dimension equals to 3 ft (0.9 m), above which pillar strength does not vary with size (Hustrulid, 1976; Bieniawski, 1983). Since it is very expensive to perform a sufficient number of in-situ large underground coal pillar strength tests, the normal procedure is to collect samples from underground and prepare small specimens for UCS tests in the laboratory. The results are then extrapolated to underground cubical pillar

strength. Step 2 is the determination of the actual pillar strength, considering the width-to-height ratio (shape effect) and using the selected pillar strength formula. Finally in step 3, the factor of safety is determined.

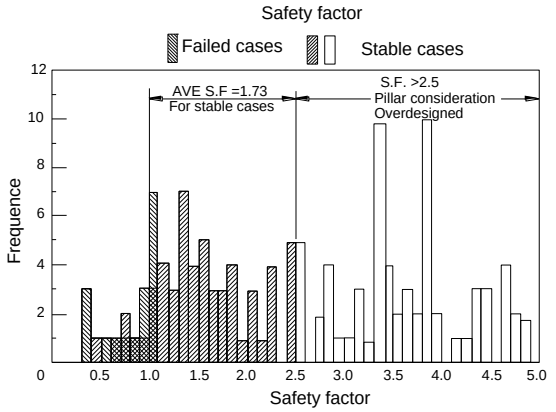

Fig. 5.3.1 Histogram of safety factors (SF) for the Bieniawski formula (Bieniawski, 1983)

A. Step 1, size effect

(1) Perform a sufficient number of UCS tests using 2-6 in. (50.8-152.4 mm) cubical coal specimens and calculate the average UCS.

(2) Substitute the average UCS and specimen dimension into Equation 5.3.6 and obtain the *K* value.

(3) Substitute *K* into the following equations as appropriate (Hustrulid, 1976) to obtain S_{cube}, the strength of the critical cubical coal pillar.

$$S_{cube} = \frac{K}{\sqrt{36}} \qquad \text{when H > 36 in. (0.9 m)} \qquad (5.3.13)$$

$$S_{cube} = \frac{K}{\sqrt{H}} \qquad \text{when H < 36 in. (0.9 m)} \qquad (5.3.14)$$

B. Step 2, shape effect

Substitute S_{cube} into Equation 5.2.1 or 5.3.3 – 5.35, 5.3.7, or 5.38-5.3.12, or substitute *K* into equation 5.3.6, to obtain S_p, the strength of the underground coal pillar with width *W* and height *H*.

C. Step 3, factor of safety

Check the factor of safety by dividing the strength by the expected applied stress and see if it meets the factor of safety for the selected formula as recommended by the developer of the strength formula.

3. Effect of Pillar Cross Section on Pillar Strength

Underground coal mine pillars assume three different shapes: square, rectangular, and parallel-piped (or diamond–shaped). All the pillar design formulae assume either square pillar or only the least dimension in rectangular and parallel-piped pillars. In other words, in a rectangular pillar the longer dimension is considered to have no effect. This is not completely true.

There are two approaches to account for the effect of the longer dimension in a rectangular or parallel-piped pillar. The first method is to use the pillar strength formulae that include the pillar length as a parameter, including Mark-Bieniawski (Mark and Chase, 1997), Stacy and Page (1986), and the Galvin-Salamon (Galvin et al., 1999) formulae. The second and more popular approach is to convert the cross-sectional area of a rectangular or parallel-piped (or diamond-shaped) pillar into a square pillar of equivalent strength, the **effective width**, W_{eff}, of which is used for the pillar width in Equations 5.3.1-5.3.12. For instance, Salamon and Oravecz (1976) suggested the following conversion factor,

$$W_{eff} = \sqrt{W_w W_\ell} \tag{5.3.15}$$

where W_{eff} is effective pillar width, W_w and W_ℓ are width and length of a rectangular pillar.

Hsiung and Peng (1985a) performed parametric analyses using a 3-D finite element technique and concluded that:

A. If pillars have the same cross sectional area, the rectangular pillars are less stable than the square pillars.

B. Pillar width rather than pillar length is the controlling factor in determining the strength of a rectangular pillar. The strength of a rectangular pillar increases with both increasing pillar width and pillar length. But, the rate of increase with increasing pillar length is insignificant in comparison with increasing pillar width.

C. For a longwall gateroad chain pillar system, a rectangular pillar can be converted into a square pillar of equivalent strength by

$$W_{eff} = W_w^{0.85} W_\ell^{0.15} \tag{5.3.16}$$

Wagner (1980) suggested that the effective width of a rectangular pillar is

$$W_{eff} = 4A_p/U \tag{5.3.17}$$

where A_p is the area of the pillar and U is the pillar circumference.

Stacy and Page (1986) recommended the following pillar strength formulae

$$\text{For } \frac{W}{H} < 4.5 \qquad S_p = K \frac{W_{eff}^{0.5}}{H^{0.7}} \text{ (MPa)} \tag{5.3.18}$$

$$\text{For } \frac{W}{H} > 4.5 \qquad S_p = K \frac{2.5}{V^{0.07}} \left\{ \left[\left(\frac{R}{4.5} \right)^{4.5} - 1 \right] + 1 \right\} \text{ (MPa)} \tag{5.3.19}$$

where k is design rock mass strength taking into account weathering and joint orientation. V is volume of the pillar, W_{eff} is effective pillar width obtained by Equation 5.3.17, and

$$R = \frac{W_{eff}}{H} \tag{5.3.20}$$

It turns out that Equations 5.3.18 and 5.3.19 are similar to Equation 5.3.21 and 5.3.22.

Following an extensive pillar survey in Australia, Galvin et al., (1999) developed the following equations for Australia and South African coal mines,

For $\frac{W}{H} < 5$ $\quad S_p = 6.88\frac{\sqrt{W\Theta}}{h^{o.7}}$ (MPa) (5.3.21)

For $\frac{W}{H} > 5$ $\quad S_p = \frac{19.05\sqrt{\Theta}}{W^{0.133}H^{0.066}}\left\{\left[\left(\frac{W}{5H}\right)^{2.5} - 1\right] + 1\right\}$ (MPa) (5.3.22)

where $\Theta_o = \frac{2W_2}{W_1 + W_2}$ (5.3.23)

$$W_{eff} = W\ \Theta\ = W\ \Theta_o^{\frac{R-3}{3}} \quad (5.3.24)$$

$$R = \frac{W}{H} \quad (5.3.25)$$

$$W = W_1 \sin\theta \quad (5.3.26)$$

where W_1 and W_2 are the pillar width and length, respectively, and θ is the internal angle of the pillar. For square and rectangular pillars $\theta = 90^o$.

In many cases, coal cores from exploration drilling are available for UCS testing. Preparation of coal cores for UCS testing is much simpler and tends to meet some testing standards more easily (ASTM, 2007). Since most pillar design formulae specify cubical samples for laboratory UCS tests, the strength obtained by testing the cylindrical cores should be converted to that of cubical specimens of equivalent strength. Tests by Townsend et al., (1977) showed that results vary from seam to seam, but the data for individual seams group centers around an average line (Fig. 5.3.2); that there is a maximum difference of 30 % in strength for the smaller specimens (1.7 in. or 43.2 mm in diameter),with the greatest variation occurring for specimens with an area of 6.4 in^2 (41.2 cm^2); that this difference diminishes with increasing size; and that the bold solid line shown in Fig. 5.3.2 can be used to relate strength of cubical and cylindrical coal specimens. Note that currently there is no standard for testing cubical coal specimen. Newman and Hoelle (1993) proposed a procedure using 3 in. cubes.

Mark and Chase (1997) refined the Bieniawski formula to consider the effect of pillar length as the Mark-Bieniawski formula,

$$S_p = S_{cube}\left\{0.64 + \left[0.54\frac{W}{H} + \left(0.18\frac{W^2}{LH}\right)\right]\right\} \quad (5.3.27)$$

where S_{cube} is in-situ coal strength, W is pillar width, L is pillar length, and H is pillar height. Mark and Chase (1997) recommended that when using the Mark-Bieniawski formula, the in-situ coal strength (S_c) is assumed to be 900 psi (6.2 MPa) and there is no need to perform laboratory coal strength tests. The recommended factor of safety for the Mark-Bieniawski rectangular pillar strength formula (Mark, 1999) is

$$SF = 2.00 - 0.016\ CMRR$$

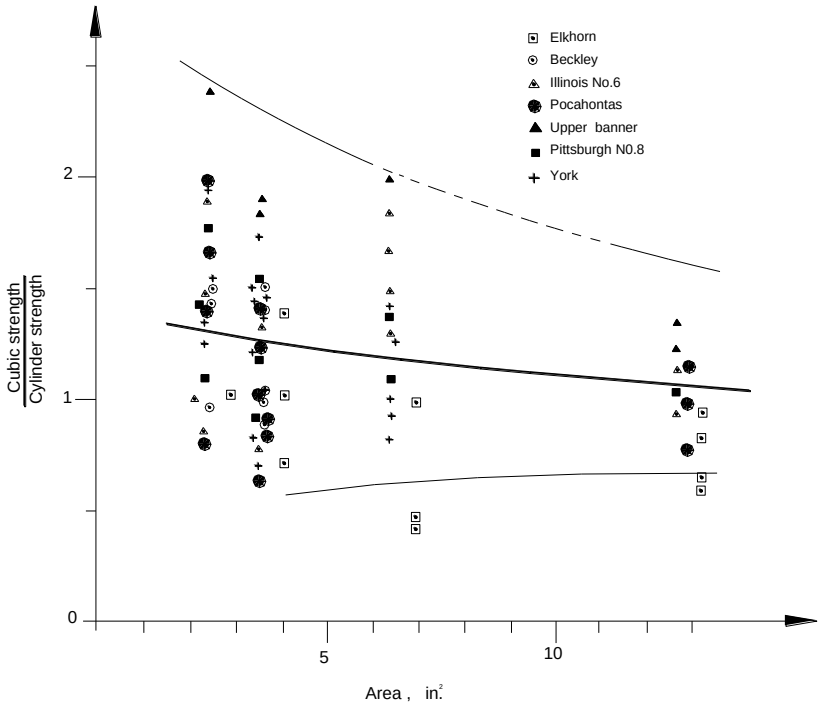

Fig. 5.3.2 Strength ratio of cubical and cylindrical coal specimens for various seams (Townsend et al., 1977; VPI&SU, 1981)

4. Comparison of Various Pillar Design Formulae

With so many pillar design methods and formulae available (Iannacchione et al., 1992; Mark et al., 1999), it is necessary to compare the differences among them, so that proper choice and/or decisions can be made for application of any selected formulae (Du et al., 2008).

Please note that in order to show the trends of differences among the formulae, some common parameters that may deviate from those recommended by the developers of the formulae were used. For instance, in cases where the developers of the formulae did not specify the cubical in-situ pillar strength, a uniform cubical pillar strength of 900 psi (6.2 MPa) was used.

A. Effect of pillar width-to-height ratio

Figure 5.3.3 is a composite plot showing the effect of width-to-height ratio (*W/H*) on pillar strength. The pillar height is kept at 7 ft (2.1 m), while the dimension of the square pillar is varied to create a pillar with *W/H* ratio ranging from 2 to 20.

All formulae predict pillar strength to increase with W/H ratio. Among all formulae, the difference in predicted strength increases with increasing *W/H* ratio.

Up to the point where $W/H = 12$, the Greenwald formula predicts the highest strength. For $W/H < 10$, the linear formulae by Bieniawski (1992), Bunting (1911) and Mark-Bienawski (Mark and Chase, 1997) predict the second highest strength. When $W/H > 12$, the Galvin and Salamon formula predicts the highest strength that increases very rapidly from there on and

leads to an infinitive strength at about *W/H* = 16. This trend does not totally conform to the general concept that when the *W/H* ratio is larger than 10 - 12, pillar strength is extremely high, approaching indestructible (Holland 1973; Bieniawski 1992). However, all linear strength formulae still predict an increasing but finite strength even when *W/H* = 20. The Holland–Gaddy formula gives the lowest pillar strength regardless of *W/H* ratio.

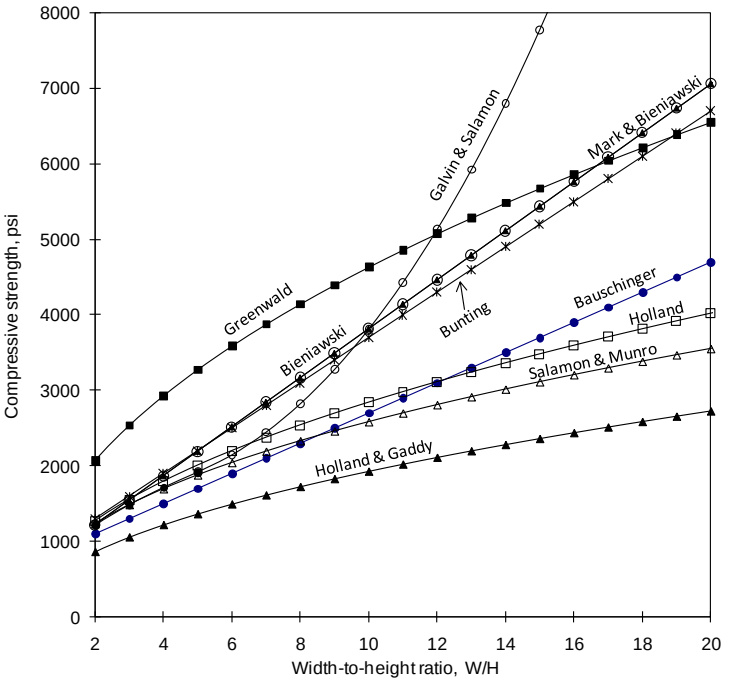

Fig. 5.3.3 Comparison of various pillar strength formulae on the effect of W/H ratio (Du et al., 2008)

Therefore, among the more popular formulae, the Bieniawski and Mark-Bieniawski formulae are the most liberal approach when *W/H* < 10, while the Holland-Gaddy is the most conservative.

B. Effect of pillar width

In this case, comparison is made using a square pillar with widths varying from 20 to 200 ft (6.1 to 61 m) in steps of 20 ft (6.1 m) (Fig. 5.3.4).

All formulae predict the pillar strength to increase with pillar width. The Greenwald formula predicts the highest strength, and the Bieniawski and Mark-Bieniawski formulae predict the second highest strength when pillar width is less than about 70 ft (21.3 m). For pillar widths greater than 70 ft (21.3 m), the Galvin and Salamon formula predicts the highest strength that increases rapidly from there on and leads to an infinite strength at around 110 ft (33.5 m). The Holland-Gaddy formula again predicts the lowest pillar strength regardless pillar width.

The linear formulae predict the strength to increase with pillar width continuously, while all other formulae also predict increasing pillar strength with increasing pillar width, but at much slower rates.

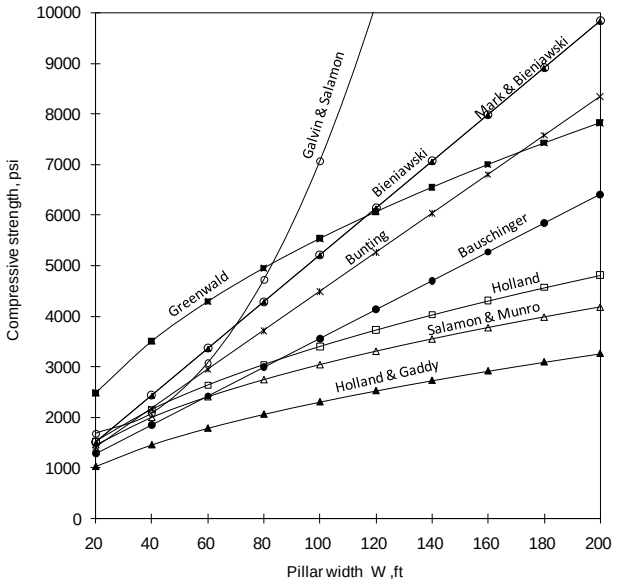

Fig. 5.3.4 Comparison of various pillar strength formulae on the effect of pillar width (Du et al., 2008)

C. Effect of pillar height

Figure 5.3.5 shows the effect of pillar height on pillar strength assuming a square pillar, 50 ft (15.2 m) wide with pillar height varying from 3 to 15 ft.

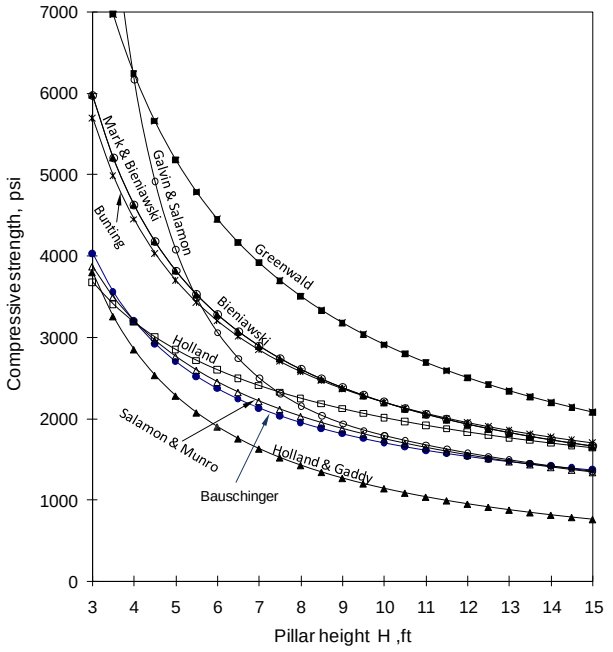

Fig. 5.3.5 Effect of pillar height on pillar strength (Du et al., 2008)

Pillar strength decreases exponentially with increasing pillar height. The rate of decrease is the largest for the Galvin and Salamon formula when pillar height is less than 10 ft (3 m). When pillar height is less than 4 ft (1.2 m), the Galvin and Salamon formula predicts an infinitive pillar strength. When pillar height is larger than 5.5 ft (1.7 m), the Greenwald formula predicts the highest pillar strength, followed by the Bieniawski, Mark-Bieniawski, and Bunting formulae. The Holland-Gaddy formula predicts the lowest strength regardless of pillar height.

D. Effect of pillar length

Only two pillar design formulae consider the length effect, i.e., The Mark-Bieniawski and Galvin-Salamon formulae. Figure 5.3.6 shows the effect of pillar length on pillar strength for various pillar strength formulae. In this case, pillar height is 7 ft (2.1 m), pillar width is 24.5 ft (7.5 m) when W/H = 3.5; pillar width is 35 ft (10.7 m) when W/H = 5; and pillar width is 56 ft (17.1 m) when W/H = 8.

Pillar strength increases with pillar length when pillar length increases from 60 to 200 ft (18.3 to 61 m). The rate of increase and W/H interval of rate increase vary with W/H ratio. For pillars with W/H = 3, the effect of pillar length on pillar strength is either minor or insignificant. For the Galvin and Salamon formula, as the W/H ratio increases to 5, strength increases slightly when pillar length increases from 30 to 90 ft (9.1 to 27.4 m). The increase is larger for the Mark and Bieniawski formula. When W/H = 8, the Galvin and Salamon formula predicts continuous increase of pillar strength with pillar length with decreasing rate of increase, while the Mark and Bieniawski formula begins to level off around 210 ft (64 m).

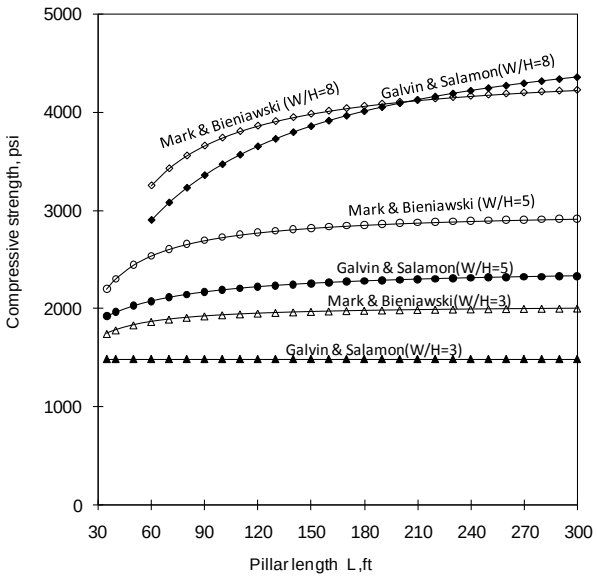

Fig. 5.3.6 Comparison of various pillar strength formulae on the effect of pillar length (Du et al., 2008)

E. Effect of shape of a pillar cross-section

The effect of shape of a pillar cross-section in plan view is recognized and discussed two ways: one is the conversion of a non-square cross-section into a square one of effective pillar width, W_{eff}. The other is to change the angle between the width and length dimensions.

Figure 5.3.7 shows the comparison of five methods as expressed by Equations 5.3.15, 5.3.16, 5.3.17, and 5.3.24 plus W_w. W_w is simply the minimum width or least dimension of the pillar dimension regardless of pillar length, as recommended by most pillar strength formulae. Fig. 5.3.8 shows the comparison of changing the angle, θ between the width and length dimensions using the Galvin and Salamon formula.

In Fig. 5.3.7, pillar length is assumed to be 100 ft (30.4 m), while varying pillar width from 0 to 100 ft (0 to 30.4 m). Equation 5.3.15 produces the largest effective width and thus the highest pillar strength, followed in decreasing order by Equation 5.3.17 and then Equation 5.3.16. The Galvin and Salamon formula gives the least effective pillar width, but increases rapidly from 20 to 60 ft (6.1 to 18.3 m) and becomes the second largest at 60 ft (18.3 m). Note all three equations (Equations 5.3.15-5.3.17) predict a larger effective width than the commonly recommended least (or minimum) width method, W_w.

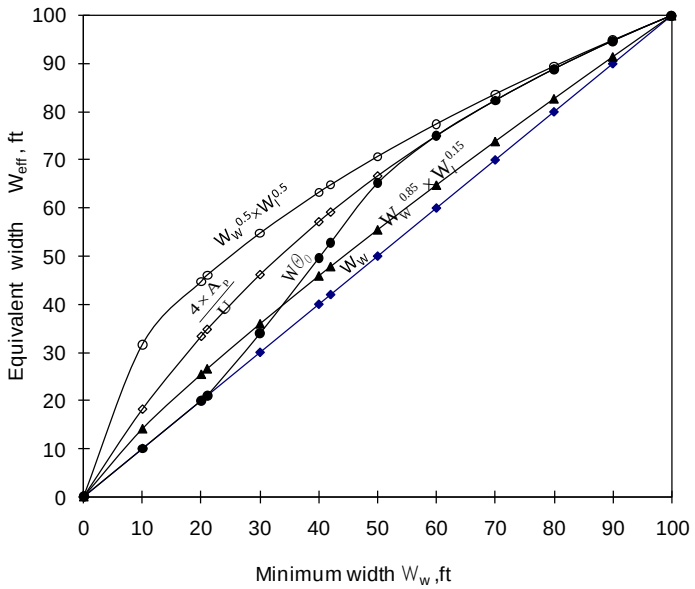

Fig. 5.3.7 Comparison of W_{eff} using the five proposed methods (Du et al., 2008)

In Fig. 5.3.8, the effect of angle θ between two side edges of the pillar is studied for three different pillar cross-sectional areas, i.e., 784, 1,225, and 2,500 ft^2 (72.9, 113.9 and 232.4 m^2). Change in pillar strength is observed by keeping the cross-sectional area constant while varying the angle θ. Note that as θ decreases from 90^0, it changes from a square pillar to a parallel-piped or diamond-shaped pillar.

Obviously, the effect of θ on pillar strength depends strongly on *W/H*. When *W/H* < 5, decreasing θ will decrease pillar strength, but the amount of decrease is not significant. On the other hand, when *W/H* > 5, decreasing θ will decrease pillar strength significantly.

Figure 5.3.9 shows that when *W/H* = 3, θ has no effect on pillar strength, and that the effect of θ on pillar strength increases with increasing *W/H* ratio.

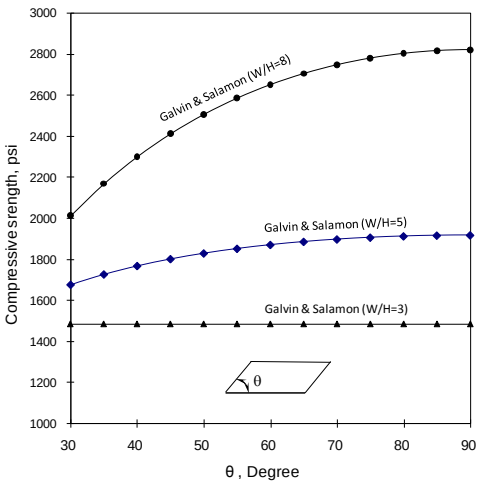

Fig. 5.3.8 Effect of θ on pillar strength according to the Galvin and Salamon formula) (Du et al., 2008

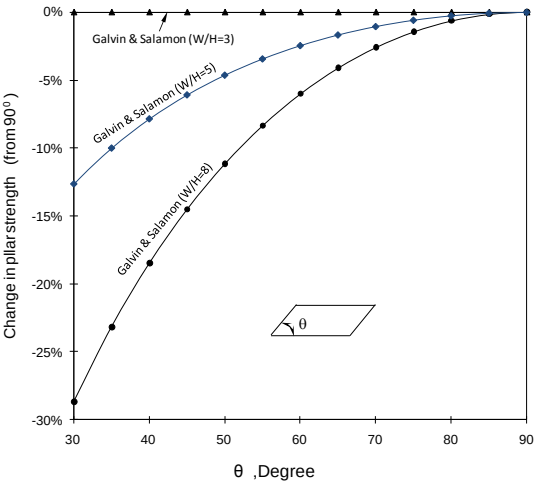

Fig. 5.3.9 Change in pillar strength due to change in θ, according to the Galvin and Salamon formula (Du et al., 2008)

6. Summary

It is quite obvious that different formulae produce different results. Pillar strengths predicted by various pillar strength formulae vary considerably, up to more than 4 times from the lowest to the highest predicted strengths. The difference grows larger as the W/H ratio increases.

It must also be emphasized that due to differences in strength, a safety factor determined for one formula is not necessarily equal to that derived for another formula, and furthermore, the recommended safety factor for different formulae are different. Thus, comparison among pillar formulae must take these factors into account.

In general, among the popular formulae, the Bieniawski and Mark-Bieniawski formulae predict the highest strength for pillars within the commonly used range. The Holland-Gaddy formula, on the other hand, predicts the lowest pillar strength, which when selected for use, provides the most conservative approach. However, everything being equal, a higher pillar strength means a smaller pillar is required and, thus, a higher coal recovery is realized.

In light of the large discrepancy, any formula may work in most situations. The key is to thoroughly understand the strength and limitation of, and the safe range of safety factors for, the formula selected.

For pillar design using empirical pillar design formula, the most important point is the selection of a proper safety factor or range of safety factors. The common approach is that once a pillar design formula is developed through tests of either in-situ underground pillars of specific coal seams or laboratory specimens, the formula is calibrated with cases of pillar failures to obtain a recommended safety factor or range of safety factors for various design purposes. In this respect the reliability and applicability of the formula selected depends on the quality of, and range of mining and geological conditions covered by, the case histories used in the calibration. The reliability and applicability of the selected formula is also highly dependent on its continuous calibration with case histories and refinements thereafter.

5.3.2 Semi-Conventional Method for a Group of Pillars

This group of pillar design method is mainly for the design of longwall gateroad chain pillar systems. The gateroad chain pillars located between two adjacent longwall panels are designed to provide safe access roads for travel to and from the longwall face prior to and during longwall retreat mining. These two- or three-row chain pillars, depending on whether the three-entry or four-entry system is used, are designed to support the abutment pressures, especially the side abutment pressure from the immediate previous panel. Consequently, the total pillar width, rather than individual pillars, is the important parameter in determining the amount of pressure that will be allowed to transfer to the current panel. Therefore, the chain pillar system should be treated as a unit.

Two design methods have been developed in this category: the analysis of longwall pillar stability (ALPS) method and the Wilson and Carr method. Both methods consider non-uniform stress distribution either from pillar external loading or from both external loading and internal stress distribution. However, they still treat all structural elements (coal, roof, and floor) as homogeneous and isotropic, and either do not or only superficially consider the effect of interaction between roof and coal and between coal and floor strata.

1. The Analysis of Longwall Pillar Stability (ALPS) Method

The only difference between ALPS and the conventional pillar design method is in the calculation of external loading (Mark, 1990).

A. Pillar loading

In ALPS, pillar loading varies considerably, depending on the location of pillars in the longwall panel, and is classified into three types: headgate loading, tailgate loading, and bleeder loading (Fig. 5.3.10).

(1) Headgate loading, L_H

Headgate loading applies to chain pillars at and around the T-junction of the headgate side of the panel being mined if the immediate previous panel has been mined. It also applies to chain pillars on both the headgate and tailgate T-Junctions if the panel being mined is the first panel in a new longwall section or new mining area (H in Fig. 5.3.10).

The headgate load, L_H, consists of the development load plus the front abutment load:

$$L_H = L_d + L_s F_h R \tag{5.3.28}$$

$$L_d = h W \gamma \tag{5.3.29}$$

$$W = \sum W_p + (n-1) W_o \tag{5.3.30}$$

$$L_s = h^2 \frac{\gamma}{2} \tan \beta \tag{5.3.31}$$

$$R = 1 - \left(\frac{D-W}{D} \right) \tag{5.3.32}$$

$$D = 9.3 h^{0.5} \tag{5.3.33}$$

where L_d is the development load, L_s is the side abutment load, F_h = 0.5 is the front abutment factor for headgate loading, R is the fraction of total side abutment load carried by the chain

pillars. *h* is depth of cover, *W* is the width of pillar system, γ is unit weight of overburden, n is the number of entries in the gate entry system, and *D* is the width of the abutment influence zone (Peng and Chiang, 1984; Peng, 2006).

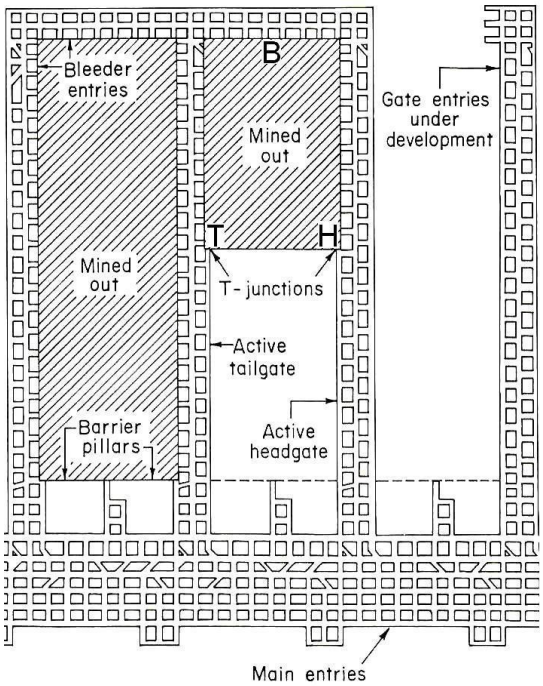

Fig. 5.3.10 Definition of headgate, tailgate, and bleeder loadings (Mark, 1990)

Side abutment is a key factor in ALPS, because the front abutment is calculated as a fraction of the side abutment. In reference to the results presented by Choi and McCain (1980), King and Whittaker (1971), and Wilson (1973), the side abutment load is represented as the wedge of strata defined by the caving angle, β = 16.6° - 21°, of the gob from the vertical. For ALPS, β = 21° is used. **Critical panels** are those whose panel width to panel depth ratio equals to 1.2-1.4. Equation 5.3.31 is for panel widths equal to or larger than the critical width. For subcritical panels, the side abutment load, L_{ss}, is

$$L_{ss} = \left(\frac{hp_w}{2} + \frac{p_w^2}{8\,tan\beta} \right) \gamma \tag{5.3.34}$$

where p_w is panel width.

The side abutment load decreases from the edge of the panel through the gateroad chain pillar system to the solid coal block in the next panel following the equation

$$\sigma = \frac{3\,L_s}{D^3} (D - x)^2 \tag{5.3.35}$$

where *x* is the distance from the edge of the gob of the previous panel.

(2) Bleeder loading, L_B

Pillars that are expected to protect bleeder entries will be subjected to the development load and the first full side abutment (B in Fig. 5.3.10).

$$L_B = L_d + L_s R \tag{5.3.36}$$

Equation 5.3.36 also applies to barrier pillar load.

(3) Tailgate loading, L_T

Being adjacent to the previous longwall gob, tailgate load (T in Fig. 5.3.10) is the most severe longwall service loading experienced during retreat mining of the second and subsequent panels. Tailgate loading consists of the development load, the first side abutment, and the second front abutment,

$$L_T = L_d + L_s + F_t L_s \tag{5.3.37}$$

where $F_t = 0.7$ is the front abutment factor for tailgate loading.

B. Pillar strength

For ALPS, the Bieniawski formula, Equation 5.3.12, is adopted, except that according to Mark and Chase (1997), in-situ coal strength (S_c) is 900 psi (6.21 MPa) and laboratory coal strength tests are not recommended.

C. Stability factor, SF

The stability factor in ALPS is the load-bearing capacity of the pillar system, B, divided by the design loading, L, or

$$SF = B/L \tag{5.3.38}$$

where L is either Equation 5.3.28, or 5.3.36 or 5.3.37 for headgate or bleeder or tailgate loading, respectively, and

$$B = \sum B_p = \sum_{n=1}^{n} \frac{S_p W_p W_\ell (144)}{W_\ell + W_o} \tag{5.3.39}$$

where B_p is the pillar load of each pillar in the pillar system, n is the number of pillars, and W_ℓ is pillar length.

Calibration with the original case histories (Fig. 5.3.11) led to the recommendation of stability factors 1.0-1.3 for use with ALPS. Later through back-analysis of more case histories (Mark and Chase, 1997), the proper stability factor for use with ALPS is changed to 1.76-0.014 CMRR. In other words, the stronger the roof, the smaller the size of the chain pillar that is required. The stability factor recommended above depends upon roof quality. This is because the goal of ALPS is really to provide a serviceable tailgate, not ensure the stability of the pillars themselves. Note that the headgate and tailgate front abutment factors may vary with mine site, because in case studies of western coal mines, JS. Chen et al., (2002) found that F_t was far greater than the recommended $F_t = 0.7$, while F_h was far less than the recommended $F_h = 0.5$.

2. Carr and Wilson's Method

This method, first proposed by Carr and Wilson (1982), is designed originally for a four-entry gateroad pillar system. In this system, the three rows of chain pillars are made of two yield pillars on the sides and an abutment pillar in the center, or as it commonly called, the yield-abutment-yield system, this system of gateroad chain pillar design was very popular in the 1980s and 1990s. Since the late 1990s, however, the industry trend of switching to a three-entry chain pillar system for faster rates of gateroad development, interest in the four-entry development system has rapidly declined. Today, only a few deep longwalls in the eastern coal field employ it mainly for ventilation and floor and bump control purposes.

Wilson's (1973) theory of pillar design is credited with the introduction of the concept of confinement in pillar design. The higher the confinement is, the higher the pillar strength.

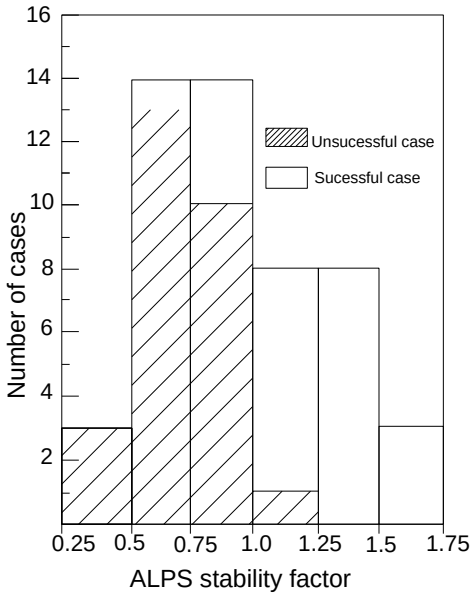

Fig. 5.3.11 ALPS stability factors (SF) calculated for the first set of case histories (Mark, 1990)

As soon as a pillar is formed, two zones develop; an outer yield zone and an inner elastic core. The yield zone has failed and cannot take any more loads, but it provides confinement to the inner core. Immediately after development, the highest stress is located at the boundary of the yield and core zones. As the longwall progresses and additional loadings are induced, stress at the core also increases continuously until it equals the highest stress at the yield/core boundary. This is the limit of roadway stability (LRS), below which both pillar and roadways surrounding it are stable. Further loading on the pillar will cause the yield zone to expand at the expense of the inner core, resulting in increased horizontal stresses that can damage the roadways surrounding it. When loading increases to such that the core is completely yielded, any additional loads will be transferred to adjacent pillars. This is the ultimate limit (UL).

A. Pillar loading

The total initial average pillar stress, σ_p is equal to average abutment stress, σ_A and overburden stress, σ_v (Mark, 1990), i.e.,

$$\sigma_{\mathrm{p}} = \sigma_{\mathrm{A}} + \sigma_{\mathrm{v}} \tag{5.3.40}$$

where

$$\sigma_A = \frac{\sigma_{max} - \sigma_v}{x_2 - x_1}\left[c\left(e^{\frac{-x_1}{c}} - e^{\frac{-x_2}{c}}\right)\right] \tag{5.3.41}$$

$$\sigma_{max} = k\,\sigma_v + S_1 \tag{5.3.42}$$

$$L_c = \frac{L_s}{\sigma_{max} - \sigma_v} \tag{5.3.43}$$

$$L_s = 0.15\,\gamma\ h^2 \tag{5.3.44}$$

where $\sigma_{\max}$ is the peak abutment stress (lb/ft^2), S_1 is intact coal strength (psf), L_s is side abutment load (lb), and k is triaxial stress factor,

$$k = \frac{1+\sin\phi}{1-\sin\phi} \tag{5.3.45}$$

where ϕ is the angle of internal friction (degree).

B. Pillar strength

Two ultimate loading (UL) pillar strength equations are provided: one for rigid roof and floor (RRF) and the other for yielding roof and floor (YRF). But only YRF is used, because under RRF, the ultimate loading is too high (Mark, 1990):

$$X_b = \frac{H}{2}\left[\left(\frac{\sigma_v}{S_1'}\right)^{\frac{1}{k-1}} - 1\right] \tag{5.3.46}$$

$$LRS = 8(Y_1) + 2\,(Y_2) + 3\,(Y_3) + Y_4 \tag{5.3.47}$$

$$UL = 8\,(Y_1) + 2(Y_2) \tag{5.3.48}$$

where

$$Y_1 = \frac{HS_1'}{2}\left[\frac{\left(\frac{2X_b}{H}+1\right)^{(k+1)} - 1}{(k+1)\frac{2}{H}} - X_b\right] \tag{5.3.49}$$

$$Y_2 = (W_\ell - 2X_b)\left(\frac{HS'_1}{2}\right)\left[\left(\frac{2X_b}{H}+1\right)^k - 1\right] \tag{5.3.50}$$

$$Y_3 = (W_p - 2X_x)\left(\frac{HS_1'}{2}\right)\left[\left(\frac{2X_b}{H}+1\right)^k - 1\right] \tag{5.3.51}$$

$$Y_4 = (W_\ell - 2X_b)(W_p - 2X_b)(k\sigma_v + S_1) \tag{5.3.52}$$

where S_1' the uniaxial compressive strength of fractured coal (psf), and W_ℓ is pillar length (ft).

C. Transfer load for roadway stability

In lieu of determining the factor of safety, the amount of load transfer due to pillar yielding is determined. The first step is to compare the total load on the pillar nearest to the gob of the immediate previous panel with its bearing capacity. If the applied load is less than the LRS, no load transfer will occur and the adjacent entry/crosscut will be stable; if the applied load is greater than LRS, but less than UL, the adjacent entry/crosscut may be damaged, but no load will be transferred; and if the applied load is greater than the UL, the additional load, called transferred remnant load (TRL), is transferred to the pillar in the next row. This process of analysis is repeated for the pillar in the next row, except that any TRL from the previous panel must be added to the total initial pillar load.

The recommended design criterion is that the TRL from the tailgate row of pillars should be less than 10,000 ton/ft along the length of the tailgate in order to avoid damage to the tailgate. When TRL is 10,000-20,000 tons/ft, damage to the tailgate will be more severe and supplementary supports will be required. When TRL is 20,000-30,000 tons/ft, damage is severe, and extensive supplementary supports are required (Carr and Wilson, 1982).

In reviewing the application of yield-abutment-yield pillar system in the Blue Creek seam, Carr (1992) stated that an abutment pillar with safety factor = 1 does not stop stress from the first longwall being transferred onto the tailgate of the second face, and that the stress on the second face tailgate due to the first face ranged from 117 to 254 tons/ft^2 when pillar size was 180 to 360 ft (54.9-109.8 m) centers under 1,400-2,200 ft (426.8-670.7m) of cover.

5.3.3 Mine Structure Modeling

Mine structures refer to the layout of entries, crosscuts, and pillars as developed. It ranges from a few pillar blocks to a section or panel or to the whole mine. In an underground coal mine, pillars are arranged in a regular pattern such that pillar loading varies with pillar location and size of the panel, while pillar strength varies with all the factors described in Section 5.2 (p. 229). Mine structure analysis through numerical computer modeling can account for all those factors and represents the most advanced technique in ground control, including pillar design.

Mine structure modeling in 2-D analysis began in early 1970s (Crouch and Fairhurst, 1973) and developed into 3-D finite element modeling in the early 1980s (Peng et al., 1980; Peng and Su, 1980). Back then, modeling was rudimentary due to very limited computer memory and slow computing speed. For 3-D longwall analysis, the finite element size was very coarse and the element size was up to 100 ft (30.4m) for one gateroad chain pillar (Hsiung and Peng, 1985a). As computer technology continued to develop, so did the science of ground control modeling.

Researchers in ground control during the last three decades identified many other factors that can affect pillar strength and stress distribution within the mine structure. Accordingly, mine structure analysis is also getting more complicated and requires more computer memory and faster computation speed.

Mine structural analysis for pillar design ranges from a single pillar system to full panel or section layout. Structural analysis is best conducted in conjunction with in-situ pillar stress monitoring to confirm the model (Gale and Mills, 1992). An example of structural analysis employing the finite element modeling is illustrated by Su and Hasenfus (1992 and 1996). The 2-D, three-panel finite element model covering the strata from the floor to surface was used. Input parameters included coal and rock strength for each stratum (i.e., elastic constants or nonlinear stress-strain characteristics, cohesion, and internal friction angle), magnitude and

orientation of in-situ horizontal stress, deformation characteristics of the gob, location of the overburden slip/shear horizons, and their frictional characteristics.

Figure 5.3.12 shows the effect of three cases of interface characteristics between roof and coal and between coal and floor: steel platens with coal seam strength 740 psi (5.1 MPa), steel platens with coal seam strength 1,000 psi (6.9 MPa), and coal/strong rock interface with zero cohesion and coefficient of friction = 0.25. With strong roof and floor, pillar strength is higher than that with machine platen loading when the width-to-height ratio is larger than 3. But the difference gradually reduces and diminishes at width-to-height ratio of 16. If the coefficient of friction is reduced due to the presence of moisture or slickensided interfaces, pillar strength will be smaller and the curve of strength versus the width-to-height ratio would approach linear due to release of constraints. Using the same models, the predicted pillar strengths correlate well with five failed pillars in two longwall gateroad systems for two mines: one is a four-entry gateroad with 30-80-30 ft (9.1-24.4-9.1 m) chain pillars, and the other is a four-entry system with 78-82-32 ft (23.8-25-9-8 m) chain pillars (Fig. 5.3.13). The measured peak strength for the failed 30 ft (9.1 m), 32 ft (9.8 m), 80 ft (24.4 m), and 82 ft (25.9 m) pillars were 6,500 psi (44.8 MPa), 4,300 psi (29.7 MPa), 8,900 psi (61.4 MPa), and 8,500 psi (58.6 MPa), respectively.

For a detailed description of mine structural analysis using numerical computer modeling, refer to Chapter 12, Computer Modeling (p. 554).

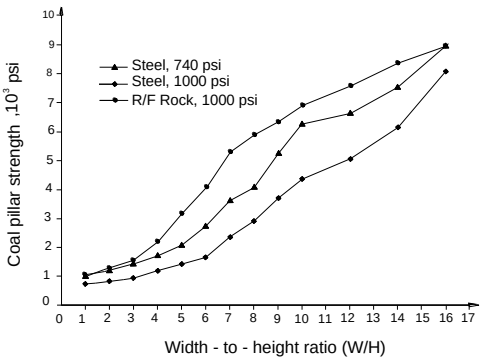

Fig. 5.3.12 Coal pillar strength versus width-to-height ratio (Su and Hasenfus, 1996)

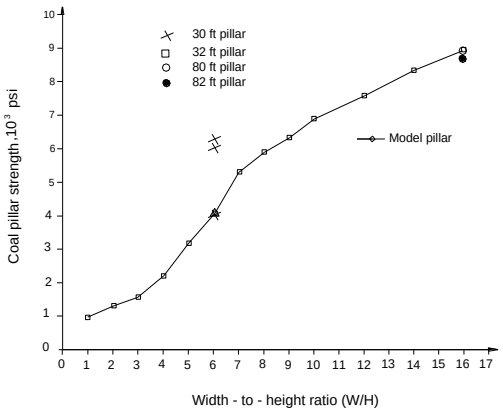

Fig. 5.3.13 Comparison of peak strength between model and failed pillars (Su and Hasenfus, 1996)

5.3.4 Determination of Pillar Strength through Instrumentation

Underground coal pillar strength has also been determined by back-analysis of tributary pillar load plus measurements of pressure change history throughout the pillar's service life (Maleki, 1981 and 1988; Skelly et al., 1977). Maleki (1981) used the spilt-platen technique to obtain complete load-deformation curves for the Upper Hiawatha seam, while Skelly et al., (1977) used vibrating-wire stress meters to obtain a complete load deformation curve for the Sewell seam. Borehole pressure cells (BPC) were also used (Campoli et al., 1993).

Figure 5.3.14A shows the average peak pillar strength for seven coal seams in eight coal mines across the U. S. (Maleki, 1992). Dashed lines are extrapolation of the data. Measurements of the stress change history of underground coal pillars during their service life unequivocally support the conclusions that underground coal pillars are able to support much larger stresses than the strength estimated by most pillar design formulae (Campoli et al., 1993; Maleki et al., 2003b). Fig. 5.3.14B includes lower bound (LB) weak geological conditions and shows that coal pillars can sustain maximum stresses between 2,500 and 4,700 psi (17 – 32 MPa) depending on structural and confining effects (Maleki, 2008). Therefore, the pillar design formulae presented previously provide a conservative estimate of pillar strength for well-cleated coals, and underestimate the pillar strength by approximately a factor of 2 for coals with no persistent cleats (Maleki and Moon, 1988).

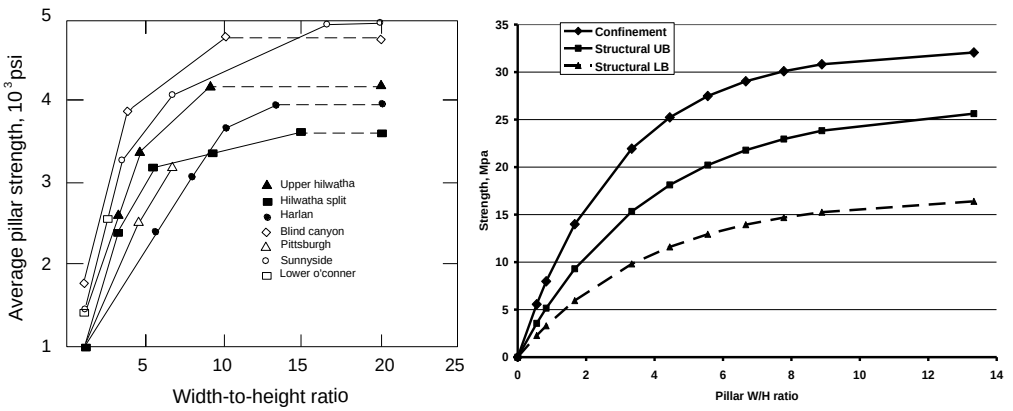

Fig. 5.3.14 Average in-situ coal pillar strength in selected U.S. coalfields (Maleki, 1992 and 2008)

Iannacchione and Mark (1992) analyzed 34 pillar stress distribution profiles measured with vibrating wire stressmeters, borehole pressure cells and borehole platened flatjacks for a distance x, up to 4 times pillar height H, into the pillar, i.e., $x/H = 4$. They found that stress gradient within the yield zone is approximately linear and that stress near the ribline is relatively high. The average pillar stress gradient can be expressed by

$$6.1\left(0.44 + 0.56\frac{W}{H}\right) \tag{5.3.53}$$

If pillar stresses cannot exceed the level attained at $x = 4H$, then pillar strength in excess of $\frac{W}{H} = 8$ is

$$\sigma_v = \frac{\left(85W^2 - 655WH + 17H^2\right)}{W^2} \tag{5.3.54}$$

Equation 5.3.54 is also shown in Fig. 5.3.15.

Tadolini and Zhang (2007) instrumented the longwall panel coal block during a pre-driven recovery room operation. Fig. 5.3.16 shows the detail of the loading of the panel coal block (or fender pillar) for the last 50 ft (15.2 m) of face advance. When the face was about 30 ft (9.1 m) from the recovery room (i.e., the fender pillar was 30 ft or 9.1 m wide), pillar loading increased rapidly and reached the peak stress of 7,500 psi (51.7 MPa) at 21 ft (6.4 m). At this time the inby side began to yield such that the panel coal block became an isolated fender pillar. At 21 ft (6.4 m) distance, the pillar load began to drop. At 15 ft (4.6 m) distance, pillar load dropped rapidly and vanished at 11 ft (3.4 m) distance, i.e., the fender pillar lost its bearing capacity completely.

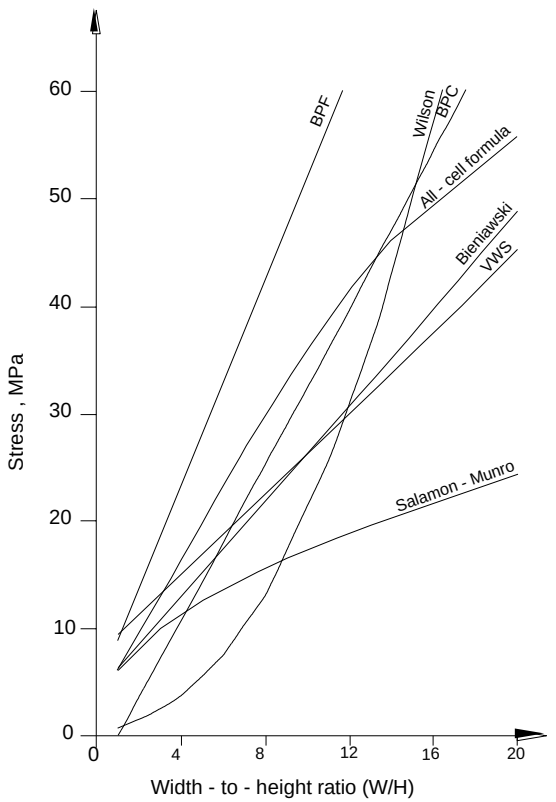

Fig. 5.3.15 Comparisons of pillar strength obtained from stress measurements with pillar strength formulae (Iannacchione and Mark, 1992)

Borehole penetrometer has also been used to determine the in-situ coal strength by Unrug et al., (1995). The results showed that the intact coal strength is 4,536 psi (31.3 MPa) for Alma seam as compared to 2,977 psi (20.5 MPa) obtained by uniaxial compressive tests in the laboratory.

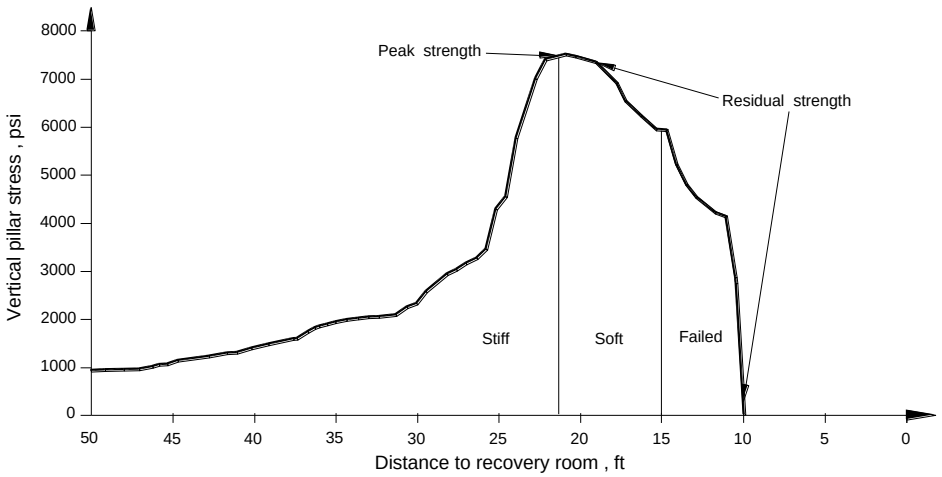

Fig. 5.3.16 The behavioral zones and vertical stress measurements for the remaining 50 ft of the fender pillar (Tadolini and Zhang, 2007)

5.4 YIELD PILLARS

5.4.1 Introduction

Yield pillars were originally designed for deep mines. If stiff pillars were to be used for deep mines, they would have to be very large such that the extraction ratio would be small and mining would not be viable (Alder et al., 1949). Yield pillars are much smaller than stiff pillars. They are designed to yield as loads are applied to them, whereas stiff pillars resist and support full loads.

Thus, a yield pillar is designed to deform progressively during its service life, thereby transferring its load to adjacent stiffer pillars or abutments and controlling the stress distribution around the openings. Ideally a yield pillar will yield at the proper time and rate depending on the characteristics of the surrounding strata and stages of mining. However, researchers differ in opinion about when the initial yielding of a yield pillar should occur and at what rate of yielding with respect to the stage of mining. For instance, some define yield pillars as those that yield or fail upon isolation from the coal seam during development (Carr et al., 1984 and 1985; Gauna et al., 1985; Mark, 1990; Tadolini and Haramy, 1992), while others state that yield pillars are those that yield completely before the maximum load arrives (Pen, 1994) or that the time and rate of yield should depend on the immediate roof quality (DeMarco, 1994).

Yield pillars were employed originally to preventing coal bumps and are being universally adopted for the two-entry longwall gateroad chain pillar system in the Utah coal fields (Peperakis, 1958; Agapito et al., 1988). For bump prevention purposes, yield pillars are 26-32 ft (7.9-9.8 m) wide, regardless of overburden depth. Experience gained from more than half a century's application of yield pillars in the Utah coal field has conclusively demonstrated that yield pillars are very effective in preventing coal bumps in gateroad chain pillars. For the history of yield pillar development in western coalfields for bump prevention, refer to Section 9.5.1 p. 448. It must be emphasized that the successful application of yield pillars in a two-entry longwall gateroad system requires a strong roof stratum that can endure a

fairly large amount of roof convergence and can endure a large roof span. In addition, proper supplementary support and adequate confinement of the sloughed coal from the yield pillars are integrated parts of successful yield pillar application.

Yield pillars have been employed in the four-entry yield-abutment-yield longwall gateroad chain pillar system in the eastern coal field in two areas: the Blue Creek seam in Alabama and the Pocahontas #3 and #4 seams in Virginia where the seams are greater than 1,200-1,500 ft (366-457 m) deep. In the Blue Creek seam, yield pillars are 20 ft (6.1 m) wide for controlling floor heave, while in the Pocahontas #3 and #4 seams, yield pillars are 30 ft (9.1 m) wide for bump control.

The three-entry, two yield pillar system has been researched for two gateroad systems (Gauna et al., 1986) in order to increase the rate of development. The total yield gateroad system allows the overburden stresses to be transferred to the adjacent panel immediately, as compared to the yield-abutment-yield system where the abutment pillar prevents significant stress transfer across the gateroad and protects the tailgate of the subsequent panel. The two rows of yield pillars and the roof were stable during and after equally sized stiff pillars. However, during the second panel mining, roof-to-floor roof span, i.e., two yield pillars, 20 ft (6.1 m) x 2 = 40 ft (12.2 m), plus 3 entry widths, 20 ft (6.1 m) x 3 = 60 ft (18.3 m), for a total of 100 ft (30.4 m).

5.4.2 Yield Pillar Design

Yield pillar design can be divided into three methods: trial-and-error, empirical, and analytical methods.

1. Trial-and-Error

The universal application of a narrow range of yield pillar sizes, 26-32 ft (7.9-9.8 m) in the Utah coalfield is a typical example of evolution through trial-and-error application for more than half a century.

2. Empirical Method – Converging Pillar Experiments

The converging pillar experiments were developed by Serata (1982), Carr et al., (1984 and 1985), and Gardner et al., (1985). This experiment uses tapering pillars in a three-entry development to produce continuous variation of yield pillar width (Fig. 5.4.1). The behavior of the tapering pillars can be divided into three qualitative distinct zones: stiff pillar, critical pillar, and yield pillar. The widest non-yielding end would reproduce the roof and floor conditions expected in normal room-and-pillar mining (i.e., stiff pillar zone), whereas the narrowest yield end would produce exceptionally high roof and floor stable conditions (i.e., yield pillar zone). Somewhere in-between these two extremes is a section of exceptionally severe damage to roof and floor strata. This section of pillars are called **critical pillars**, which is simply defined as those being too large to yield either non-violently or to yield after the roof and floor sustain permanent damage, and those are too small to support the full abutment load (DeMarco, 1996; Koehler and DeMarco, 1995).

Figure 5.4.2 shows the measured roof and floor convergences for a three-room taper pillar experiment where the stiff, critical, and yield pillars are 50 ft (m), 30 ft (m), and 15 (m), respectively. Notice the large and high rate of roof and floor convergence for the critical pillar section.

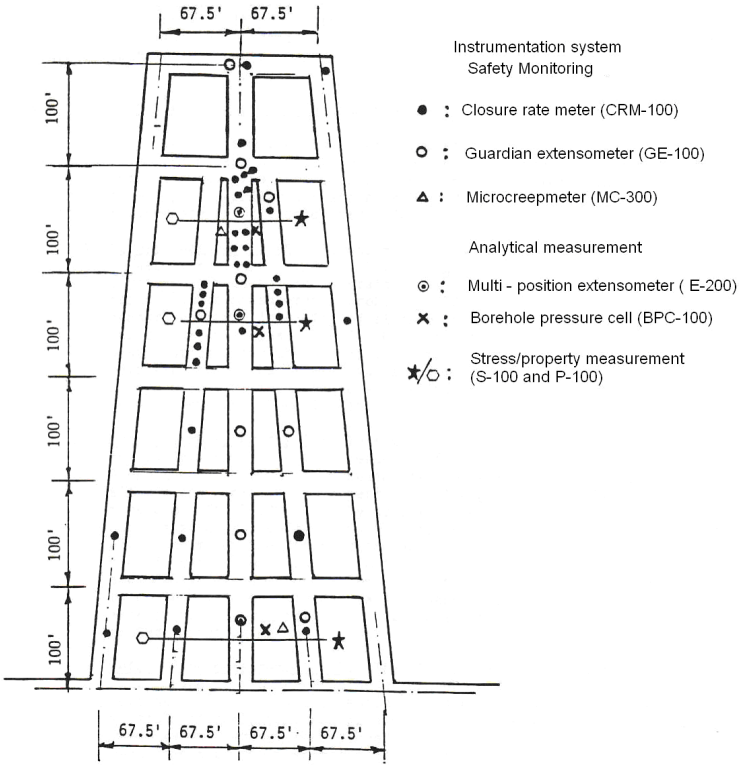

Fig. 5.4.1 An example of layout and instrument deployment of a three-room tapered pillar experiment (TPE) (modified from SGI, 1888)

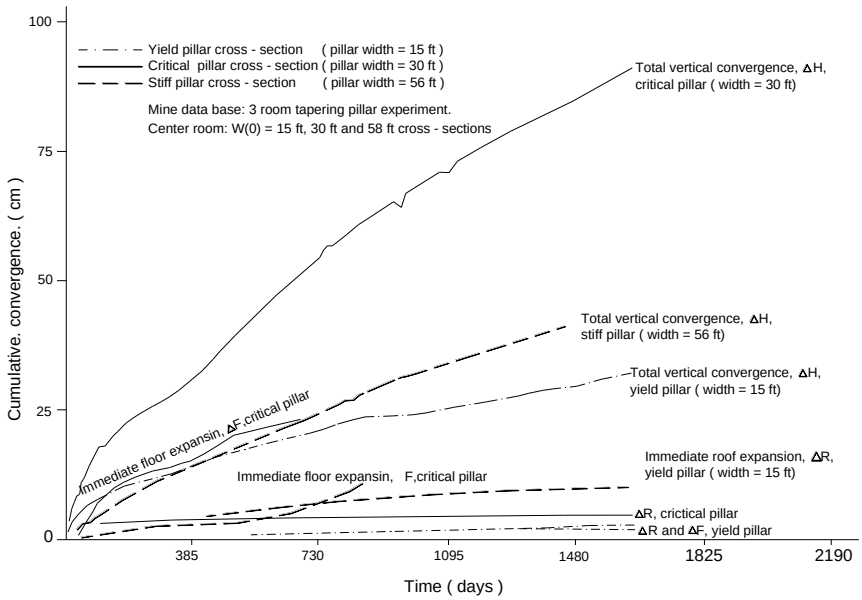

Fig. 5.4.2 Roof-to-floor convergences for stiff, critical and yield pillars (modified from Carr et al., 1985)

Figure 5.4.3 shows the measured stress distributions for a tapering pillar experiment for 80 ft (24.4 m), 40 ft (12.2 m), and 10 ft (3.04 m) pillars, respectively. The stiff (abutment) pillar is characterized by having an elastic core of low stress; the stress level reaches the highest level at the pillar center in the critical pillar; and yielding has occurred in all areas of yield pillar.

From Figs. 5.4.2 and 5.4.3, it is obvious that a yield pillar is site specific, depending on local geological conditions.

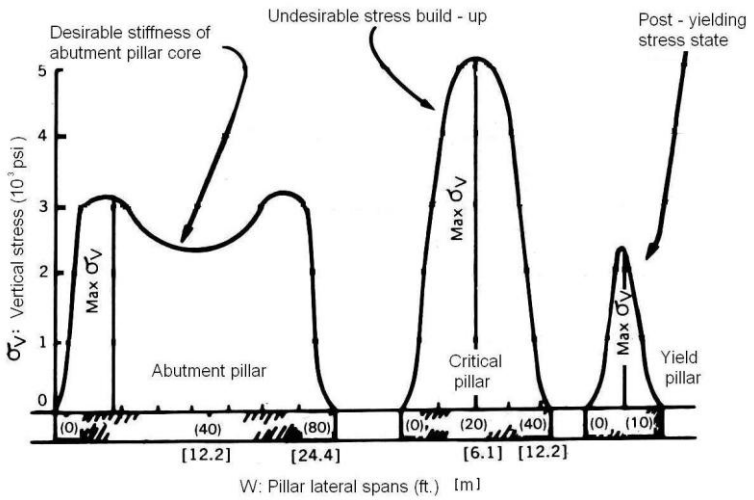

Fig. 5.4.3 Stress distribution within the stiff, critical and yield pillars (modified from Carr et al., 1985)

3. Analytical Method

Five analytical methods are available for yield pillar design (Carr and Wilson, 1982; G Chen, 1989; JS Chen et al., 1999; Tsang and Peng, 1993; and Morsy and Peng, 2003).

Wilson adapted his pillar design concept (Wilson, 1973 and 1977) to U.S. longwall multiple gateroad systems by combining both yield and abutment pillars in an integrated manner (see Section 5.3.2, p. 253). Using Equation 5.3.46, the yield width of a pillar was determined initially to be from 23 to 34 ft (7.0 to 10.3 m) for the Blue Creek seam in Alabama. The decision was made to begin experimenting with 25 ft (7.6 m) wide pillars. The results of underground monitoring (Brasfield and Hendon, 1994) led to the development of an additional experimental area with 20 ft (6.1 m) wide pillars, which proved to be appropriate for the Blue Creek seam (Gauna et al., 1985). The 20 ft (6.1 m) yield pillars in the four-entry yield-abutment-yield pillar system has been the industry standard ever since.

Chen (1989) defined the yield pillar as a pillar without an elastic core. He combined numerical modeling and Wilson's confined core concept to define three types of yield pillar widths:

A. The maximum (critical) yield pillar width is twice the width of the yield zone, W_{max},

$$W_{max} = 2X_b = H\left\{9.61\cos\left[\frac{1}{3}\cos^{-1}\left(\frac{\gamma z 10^{-3}}{\kappa^{1.7}\left(0.17\nu^2 + 0.057\nu - 0.028\right)} - 1\right)\right] - 4.8\right\} \quad (5.4.1)$$

B. The recommended yield pillar, W_r, is defined as the pillar width in which the peak vertical stress at the center of a completely yielded pillar equals the average tributary loading stress.

$$\frac{\gamma z(W_r + W_o)^2}{W_r^2} = k^{2.7}\left(0.17\nu^2 + 0.057\nu - 0.028\right)\left[454\left(\frac{W_r}{2H}\right)^3 + 6545\left(\frac{W_r}{2H}\right)^2\right] \quad (5.4.2)$$

C. The minimum pillar width, $W_{min,}$ is the width of the yield pillar that supports the roof strata below the pressure arch.

$$\frac{2}{3}\gamma D W_t(W_{min} + W_o) = k^{2.7}\left(0.17\nu^2 + 0.57\nu - 0.028\right)\left(273\frac{W_{min}^4}{H^2} + 5.68\frac{W_{min}^5}{H^3}\right) \quad (5.4.3)$$

where $W_t = W_{min} + 2W_o$ is the width and $D = 2W_t$ is the height of pressure arch, respectively, W_o is the entry width, ν is Poisson's ratio, z is overburden depth, and H is pillar height.

JS Chen et al., (1999) found that for the D seam in Utah, violent failures occurred when specimens reached a UCS of greater than 4,000 psi (27.6 MPa), while non-violent failure modes were observed when the strength was less than 4,000 psi (27.6 MPa). They introduced three criteria to design the yield pillar system for bump-prone longwall mines: tailgate stability factor $\leq$ 0.18, width-to-yield zone of a yield pillar $\leq$ 1.5, and width-to-height ratio of yield pillars $\leq$ 5. If all three criteria are met, tailgate pillar bumps can be eliminated. If all three parameters are greater than their threshold values, the intended yield pillar will yield in a violent manner. If only one of the three parameters is greater than its corresponding threshold value, a tailgate bump of light significance may be possible.

Tsang (1992) and Tsang and Peng, (1993) used two-dimensional finite element models combined with fractional experiment design to develop a set of regression equations for yield pillar design for a three-entry longwall gateroad system. A three-level orthogonal design for the most significant variables was used to minimize the number of finite element models. The developed regression equations consider the relationships between the stability conditions of the entry system, i.e., roof, pillar, and floor under different geological conditions (Table 5.4.1). Based on the recommended pillar safety factor (Table 5.4.2), Tsang's method can be used to design different types of three-entry system; i.e., Stiff-Stiff (S-S), Yield-Stiff (Y-S) and Yield-Yield (Y-Y). Tsang assumed that the pillar widths estimated by the regression equations in Table 5.4.2 are initial pillar widths. These initial pillar widths should be increased in the followings cases:

1. If the roof tensile strength was less than the estimated maximum tensile stress.
2. If the floor and/or roof safety factors, were less than 1.3.

Table 5.4.2 Recommended pillar safety factors for Tsang's method

Design layout	SF (stiff pillar)	SF (yield pillar)
Stiff-Stiff (S-S)	1.3	1.3
Yield-Yield (Y-Y)	0.9	0.9
Stiff-Yield (S-Y)	1.5	0.9

Morsy (2003) developed a method for yield pillar design for bump prevention. Once a pillar is developed, three zones of different levels of confinement can be defined, i.e., core, transition and rib zones (Morsy, 2003), (Fig. 5.4.4).

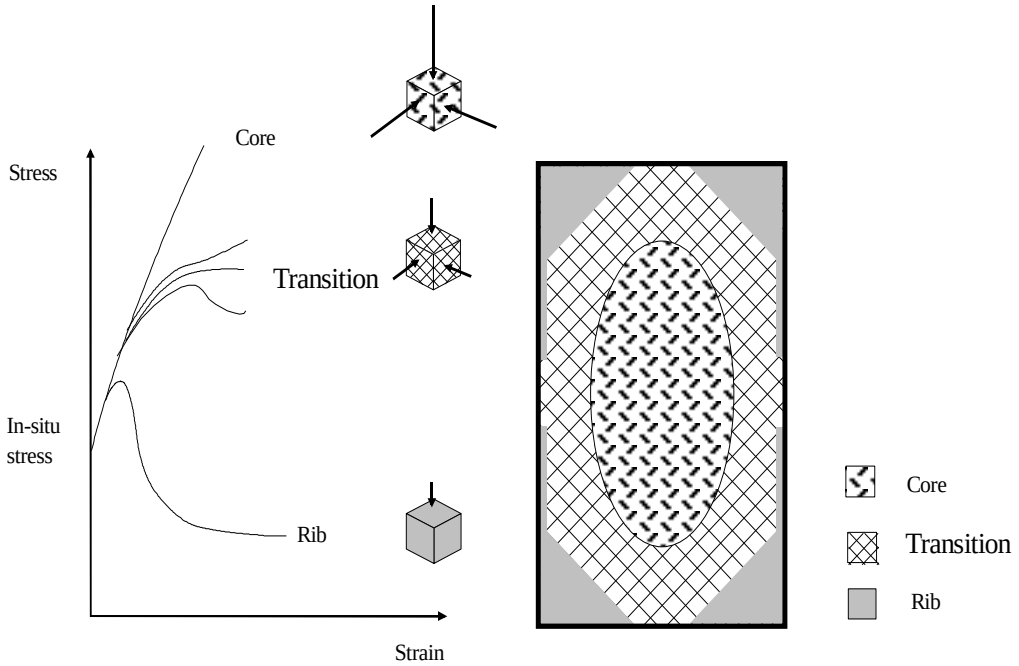

Fig. 5.4.4 View of yield pillar loading zones (Morsy, 2003)

Core zone - The core zone occupies the center portion of the pillar and is defined as the part of the pillar that does not experience any plastic deformations. The elastic behavior of the core zone is a result of confining stresses applied in this zone. Therefore, the core zone stores a significant amount of elastic strain energy.

The stability of core zone is assessed by **the core stability factor (CSF)**. The CSF is defined by the Druker-Prager yield criterion and stress level in the core zone. The core zone has the ability to store a significant amount of elastic strain energy. As long as the core stability factor CSF is greater than 1, the elastic strain energy stored in this zone will be in stable condition. This condition is obvious in the stiff pillar design, where the core zone represents most of the pillar and the stress level inside the stiff pillar is less than its yield strength. On other hand the stability of the core is crucial for the yield pillar, especially when the longwall approaches it. At that stage of mining, part of the core zone start to yield and join the transition zone. Therefore, the stored core elastic strain energy could be released to the surrounding in a violence fashion.

Transition zone – The transition zone is located between the rib and core and characterized by a wide range of confining stresses. It is the most complicated part of the pillar where three types of stress-strain behaviors could be observed in this zone, i.e., strain hardening, elastic-perfect plastic and strain-softening with high residual stress. Parts of the energy of the transition zone is dissipated in the form of plastic deformation while a significant amount of elastic strain energy is stored in this zone.

Table 5.4.1 Regression equations for different roof/floor conditions (Tsang, 1993)

	Regression equations
Strong roof and strong floor	$W_1 = \left(\frac{C}{Z}\right)^{-0.4048}\left(52.7884SF_1 - 15.4181SF_2 + 0.0005HW_p\right)$ $W_2 = \left(\frac{C}{Z}\right)^{-0.5581}\left(44.9214SF_2 - 23.1242SF_1 + 0.0005HW_p\right)$ $T_r = Z^{0.7454}\left(\frac{2.9877}{\sqrt{W_1}} + \frac{1.0168}{\sqrt{W_2}} + 2.8\times10^{-9}W_eE_r\right)$
Strong roof and weak floor	$W_1 = \left(\frac{C}{Z}\right)^{-0.4162}\left(57.1280SF_1 - 24.9814SF_2 + 1.03\times10^{3}\frac{HW_p}{E_f}\right)$ $W_2 = \left(\frac{C}{Z}\right)^{-0.4931}\left(52.9712SF_2 - 30.3162SF_1 + 1.03\times10^{3}\frac{HW_p}{E_f}\right)$ $T_r = Z^{0.6775}\left(\frac{3.7869}{\sqrt{W_1}} + \frac{1.2029}{\sqrt{W_2}} + 9.7\times10^{-9}W_eE_r\right)$ $SF_f = 2.162\times10^{-3}\left(\frac{E_f}{Z}\right)^{0.4442}\left(0.2548W_1 + 0.1403W_2 + 6.4\frac{\sigma_h}{W}\right)$
Weak roof and strong floor	$W_1 = \left(\frac{C}{Z}\right)^{-0.4135}\left(62.7666SF_1 - 22.8459SF_2 + 8.15\frac{HW_P}{E_r}\right)$ $W_2 = \left(\frac{C}{Z}\right)^{-4616}\left(62.8519F_1 - 29.7170SF_2 + 1.8\times10^{2}\frac{HW_P}{E_r}\right)$ $SFr = 2.398\times10^{-3}\left(\frac{E_r}{Z}\right)^{0.4367}\left(0.2384W_1 + 0.1217W_2 + 4.5\frac{\sigma_h}{W_p}\right)$ $T_f = Z^{0.8759}\left(\frac{1.3043}{\sqrt{W_1}} + \frac{0.4907}{\sqrt{W_2}} + 3.4\times10^{-4}W_eE_r + \frac{0.9236}{\sigma_h}\right)$
Weak roof and weak floor	$W_1 = \left(\frac{C}{Z}\right)^{-0.5235}\left(52.7862SF_1 - 15.2109SF_2 + 1.17\times10^{7}\frac{HW_p}{E_rE_f}\right)$ $W_2 = \left(\frac{C}{Z}\right)^{-0.5341}\left(53.7009SF_2 - 23.4415SF_1 + 2.02\times10^{3}\frac{HW_p}{E_rE_f}\right)$ $SF_r = 4.521\times10^{-3}\left(\frac{E_r}{Z}\right)^{0.3908}\left(0.1339W_1 + 0.1532W_2 + 6.5989\frac{\sigma_h}{W_p}\right)$ $SF_f = 2.4\times10^{-4}\left(\frac{E_f}{Z}\right)^{0.6032}\left(0.5568W_1 + 0.8454W_2 + 53.8824\frac{\sigma_h}{W_p}\right)$

where

W_1 and W_2 are pillar widths for pillar 1 and pillar 2, respectively, ft;
SF_1 and SF_2 are the safety factors for pillar 1 and pillar 2, respectively;
SF_r and SF_f are the safety factors for immediate roof and floor, respectively;
C is the cohesion strength of the coal, psi;
Z is the overburden depth, ft;
H is the pillar height, ft;
W_e is the entry width, ft;
W_p is the panel width, ft;
E_r and E_f are the Young's module of the immediate roof and floor, respectively, psi;
σ_h is the virgin horizontal stress, psi; and
T_r is maximum tensile stress in the roof, psi.

Figure 5.4.5 shows a typical stress-strain curve for the transition zone. At any stress level, σ_c, the shaded triangle CED represents the amount of stored strain energy, while the area of polygon OABCE represents the dissipated energy, W_p. The stability of the transition zone is assessed by the **bump index (BI)**. The BI is determined as a ratio of elastic strain energy stored in the transition zone to the plastic energy dissipated in the transition zone in the form of cracking and permanent deformation. The larger the bump index the more elastic energy stored in the pillar and the more tendency for serious coal bumps.

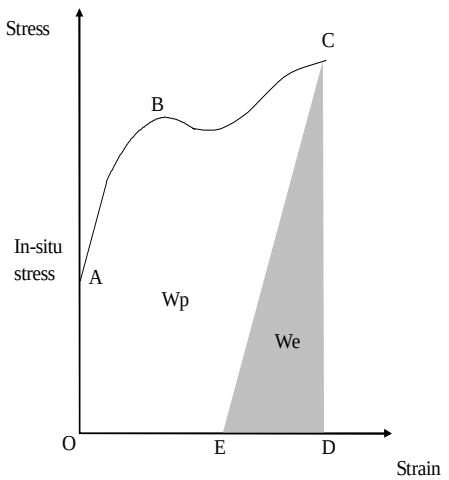

Fig. 5.4.5 Strain energy storage index, BI for the transition zone (Morsy, 2003)

Rib zone – The rib zone occupies the pillar corners and ribs. The rib zone is characterized by strain softening with low residual stress because it is bounded by free faces, i.e., low confining pressures. The pillar yielding starts from the rib zone and propagates towards the pillar core. Most of the loading energy of the rib zone is dissipated in the form of plastic deformation, e.g., rib sloughing and cracking. Therefore the Bump Index can not express the stability of rib zone.

The rib zone is defined as the part of the pillar that has a post-peak slope greater than the local mine stiffness. The stability of rib zone is assessed by the **rib instability factor** (RIF) which is the ratio between the post-peak slope and the local mine stiffness criterion. The rib zone of coal pillar is defined as the portion of the pillar that has RIF greater than 1. The **Rib Zone Ratio (RZR)** describes the ratio of the rib zone portion in the pillar to the total volume of the pillar. The larger the rib zone ratios (RZR), the larger the energy that can be released to the surrounding. The RZR covers a wide range of instabilities, from unrecognizable rib bounces to serious ones.

The size and stability of pillar zones depends on many factors, such as the end constraint provided by the roof and floor, pillar width, overburden depth, friction angle of coal and stage of mining; development, headgate and tailgate loadings. The loading condition at the longwall face is similar to the coal pillar ribs. Therefore, it is believed that the RZR could be a suitable measure to check the bump potential of longwall face.

The yield pillar is composed of a number of elements. The stability of the pillar zones is evaluated in two steps: first, the stability measure of every element inside the pillar zone is

estimated, and second, the stability of the pillar zone is calculated as an average for the stability measures of all the elements located inside the loading zone.

In the elastic core, the element stability factor (*ESF*) is defined by

$$ESF = \frac{k + J_1 \tan \alpha}{J_{2D}} \tag{5.4.4}$$

where α and k are the material property constants; J_1 is the first invariant of stress tensor; and J_{2D} is the second invariant of the deviator stress tensor. *ESF* = 1 for those elements experiencing plastic deformation or greater than 1 for the elastic elements. The *CSF* is determined by averaging the *ESF* of all elements located within the core zone. As long as the *CSF* is greater than 1, the elastic strain energy stored in this zone will be in stable condition.

The element bump index, *EBI* is calculated by (Brauner, 1994)

$$EBI = \frac{W_e}{W_p} \tag{5.4.5}$$

The bump index *BI* for the transition zone is determined by averaging the element bump indices. The larger the bump index the more elastic energy stored in the pillar and the more tendency for serious coal bumps.

The local mine stiffness criterion is used to evaluate the instability of the rib zone. The element instability factor (*EIF*) for the rib zone elements is determined by

$$EIF = \frac{\left|K_p\right|}{\left|K_{LMS}\right|} \tag{5.4.6}$$

where L_{LMS} is the local mine stiffness and K_p is pillar post-peak stiffness. The *EIF* should be greater than 1. The RIF is determined by averaging the element instability factors (*EIF*) of all the elements located in the rib zone. The larger the rib instability factors, the larger the energy that can be released to the surrounding.

5.5 BARRIER PILLARS

Functionally, there are two types of barrier pillars: internal and outcrop barriers. **Internal barrier pillars** are pillars left to support and separate mains from the mined panels, or to separate mined panels. **Outcrop barriers** are those left around the perimeter of the outcrop in the above-drainage mines. The internal barrier pillars are primarily designed to support the abutment load transferred over to them, whereas the outcrop barrier pillars, and in some cases internal barrier pillars, are not only designed to support the abutment load, but also prevent excessive water inflow from the flooded portion of the mine. There are many empirical design formulae for both types of barrier pillars (Kendorsi and Bunnell 2007; Koehler and Tadolini, 1995), several of which are discussed in this section.

For site-specific design of barrier pillars, Koehler et al., (1989) demonstrated a method using underground instrumentation data. Borehole pressure cells were used to monitor the pressure history of the barrier pillar as mining progressed. The changes in pressure distribution across the barrier pillar were used to develop the barrier pillar strength.

5.5.1 Internal Barrier Pillars

The mine inspector's formula, developed in Pennsylvania by Ashley (1930) is,

$$W_b = 20 + 4H + 0.1\,h \tag{5.5.1}$$

where W_b is the width of the barrier pillar, H is mining height, and h is depth of cover.

The barrier pillar width recommended by Dunn's Rule (Koehler and Tadolini, 1995) is

$$W_h = \frac{h-180}{20} + 15 \tag{5.5.2}$$

A rule of thumb developed and used successfully by the U.K. coal operators (King and Whittaker, 1971) is,

$$W_b = (h/10) + 45 \tag{5.5.3}$$

Based on observation in the U.S. and Canada, the North American formula for barrier pillar width (Koehler and Tadolini, 1995) is

$$W_b = \frac{hW_{panel}}{7000 - h} \tag{5.5.4}$$

where W_{panel} is the width of adjacent panel.

Since the width-to-height ratio and length-to-width ratio of the barrier pillar is usually very large, i.e., more than 8-10, the strength of the barrier pillar should be very high, according to Equations 5.3.1-5.3.12. It follows that the design of a barrier pillar should emphasize the amount of load that is allowed to be transferred over to either side of the barrier pillar when the abutment load from either side is known. In this respect, the barrier pillars designed by using Equations 5.5.1-5.5.4 will be on the conservative side. A more reasonable barrier pillar dimension can be determined by numerical computer modeling.

5.5.2 Outcrop Barrier Pillars

After a coal mine is abandoned, it is soon flooded with water. The barrier pillars designed to contain those mine waters must not only be able to support the overburden load, they should also be able to resist the water head and water seepage (Kohli and Block, 2007; Luo et al., 2001b).

If the outcrop barrier is not designed properly, pressure from a water-filled underground coal mine may cause a "blowout" or sudden release of mine pool water through the hillside above the mine. Failures may be due to roof falls, hydrostatic uplift, overtopping, or piping.

Ash and Eaton (1948) developed a barrier pillar formulae for anthracite coal of Pennsylvania,

$$W_b = 50 + 0.426\,h \tag{5.5.5}$$

The old English barrier pillar law estimates the barrier width based on hydraulic head and seam height,

$$W = \frac{HH_{hy}}{100} + 5H \tag{5.5.6}$$

where H_{hy} is hydraulic head.

A rule of thumb formula in effect in central Appalachia is (KNREP, 1994a and 1994b; VDMME, 1996)

$$W_b = P_h + 50 \tag{5.5.7}$$

where W_b is the required barrier width to resist against a hydrostatic water head of P_h.

If the material above the outcrop barrier is subjected to an uplifting force and when the water head is greater than the weight of the overburden, a blowout will occur (Kohli and Block, 2007). To prevent a blow out, barrier pillar width should be

$$W_b = \beta\ (0.385\ H + 0.48\ P_h) \tag{5.5.8}$$

where β is surface slope expressed by the horizontal over vertical distance, H is mining height (ft), and P_h is total hydrostatic water head (ft).

The most conservative approach is to assume that the wedge-shaped hill top above the outcrop barrier will fail by sliding (Kohli and Block, 2007),

$$31.2P_h^{\,2} = \left[51.3\left(\frac{W_b}{\beta}\right) + 17.6\,H\,W_b + 8.8\,\beta\,H^2 \right] tan\phi \tag{5.5.9}$$

where ϕ is internal angle of friction. Equation 5.5.9 is then solved for W_b.

5.6 MODES OF PILLAR FAILURES

The perception of pillar failures varies with the individual (Peng, 2007). Since, by definition, a coal pillar is designed to support the overburden and protect the adjacent entries/crosscuts, pillar failure simply means its failure to achieve one or both functions. Accordingly, pillar failure can be either the pillar itself or adjacent entries/crosscuts or both. Stability of entries/crosscuts is discussed in Chapter 10 (p.462).

Pillar failure ranges from sloughage of ribs to total collapse or bumps.

5.6.1 Sloughage of Pillar Ribs and Sliding of Pillar Materials

1. Failure Characteristics

Depending on cover depth, mining or pillar height, and partings characteristics, sloughage of pillar ribs will occur and range from minor to severe. Obviously, minor rib sloughage will not pose any effect on pillar stability. However, rib soughing frequently progresses with time and if supports are not properly and timely installed, severe rib sloughing will lead to pillar deterioration to such an extent that pillars cannot serve their designed functions. Conversely, for yield pillars, rib sloughage in various degrees is expected due to pillar yielding.

As stated in Section 5.2.2 (p. 231) different organic groups in coal or macerals respond differently to stress environments. Figures 5.6.1 and 5.6.2 show examples of how the bright fusinite and dull vitrinite control the initial rib sloughing leading to final collapse in a pre-driven open entry (Peng, 2007, p. 288).

Inherent fractures or joints of critical orientations (see Fig. 2.6.12, p. 62) including cleat characteristics, may cause portions of the pillar materials to slide off gradually or suddenly, leading to final collapse (see Fig. 5.2.8, p. 236).

Failures are also caused by lateral dilation of a claystone layer in the mine roof, bedding plane contacts, and floor (Maleki, 1992).

2. Failure Mechanisms

Two major factors contribute to rib spalling, stress and geologic structures. As discussed in Section 3.3.1 (p.94), coal cleat systems are major contributors to rib sloughage depending on how well they are developed and the orientation of entries/crosscuts with respect to that of the cleat, especially the face cleat. Entries/crosscuts should preferably intersect the cleats obliquely, not parallel to avoid pronounced sloughing.

A pillar is formed by removing coal surrounding it. Due to the loss of confinement from the natural state, pillar ribs tend to expand laterally, depending on the overburden load, pillar width-to-height ratio, and the properties of interfaces between roof and coal and coal and floor strata. This lateral expansion is the major cause of pillar sloughing, and its severity increases with increasing pressure during its service life, as shown in Fig. 5.6.2.

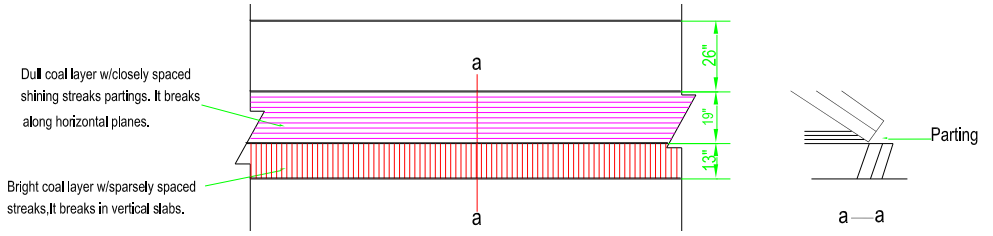

Fig. 5.6.1 Cross-section structure of Eagle seam, looking into pillar rib (Peng, 2007)

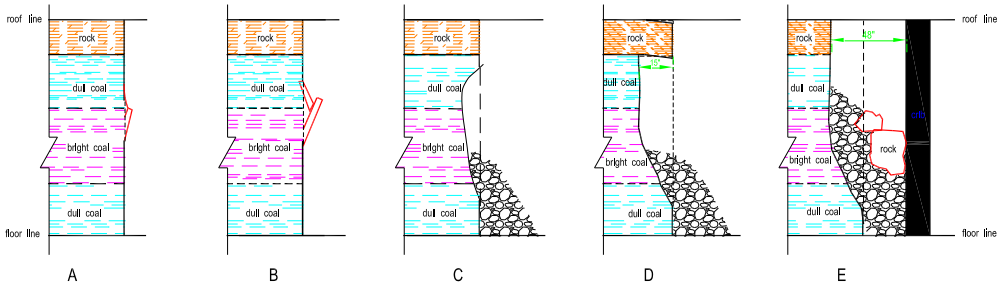

Fig. 5.6.2 Stages of rib sloughing as the longwall front abutment pressure approaches (Peng, 2007)

5.6.2 Pillar Collapse

1. Failure Characteristics

Pillar collapse or squeeze occurs when a critical stage of mining is attained, depending on a combination of pillar size, mining dimension (or section/panel size), and overburden stratigraphic sequence (see Fig. 5.2.9). There are three possible scenarios for pillar collapse: (1) in most cases, it initiates suddenly in a local area and propagates outward gradually with time; (2) it occurs suddenly and stops in the local area; and (3) it initiates and propagates gradually (Chase et al., 1994; Peng, 2007; Luo and Peng, 1997a; van der Merwe, 2006; van der Merwe et al., 1999). Mark et al., (2003) defined pillar collapses as pillar failures that occur rapidly when pillar width-to-height ratio is 3 or less, while pillar squeeze is a gradual process. Pillar collapse or squeeze may involve a few to several thousand of pillars.

The general features of underground massive pillar failures are (Fig. 5.6.3) (Peng, 2007):

A. The roof converges suddenly from less than one to three feet (0.3-0.9 m) in a large area, but remains intact. Thereafter, it may propagate slowly or may not. Roof falls may occur in a few areas.

B. Roof convergence is accompanied by failures of pillars in the form of rib sloughage of various degrees or depths. Rib sloughage occurs at the upper portion of the pillar starting from the coal/rock interface downward. The broken coal fragments from rib sloughage fall on the mine floor immediately adjacent to the coal pillar from which they sloughs off. Those fragments pile up to various heights, the highest being immediate to the coal pillar and decreasing away from it. These coal fragments may or may not overlay those from the opposite rib. Those fragments, however loose they may be, provide some confinement to the coal pillar and contribute to the stability of the sloughed pillars, preventing them from being completely crushed out.

C. The floor may or may not heave.

It is interesting to note that the failures of stiff pillars documented in this chapter are similar in form to those of yield pillars discussed in Section 5.4 (p. 259). The only difference is that in yield pillars, rib spalling is intentional but controlled to within the operation and safety limits during their effective service life.

Fig. 5.6.3 Typical pillar collapse. Both ribs sloughed off severely, followed by moderate skin falls. The debris piles from both ribs met at the entry center (Peng, 2007)

2. Failure Mechanisms

Various theories have been proposed to explain the causes of pillar collapse or squeeze. The most common approach is to prove that the strength of an individual pillar has been exceeded, thereby transferring its load to neighboring pillars, which in turn transfer the load to other neighboring pillars. This process continues until it is stopped when the total load (i.e., transferred load + original pillar load) is less than the pillar strength. This process is called **pillar cascading failure (PCF)** or domino effect.

Study of cases of massive pillar collapses shows that pillar squeezes or collapses can occur in either pillaring sections (Chase et al., 1994; Khair 1986; Mishra and Grayson, 1981; Morsy and Peng, 2002a; Tang and Peng, 1985 and 1990) or development sections (Artler, 1985; Tang and Peng, 1985; Zingano et al., 2004 and 2005) and that massive pillar squeezes or collapses started only when a section or a mined area reaches a certain size and displays characteristics of mining and geological conditions on the site of interest. Consequently, it is the combination of pillar strength (or more exactly, pillar dimension), area mined (or section dimension), and roof and floor strata characteristics. In other words, the load shedding domino

effect in massive pillar failure does not occur only due to insufficient pillar strength, but also because of the roof strata quality above the mined area, since the load is first imposed by and, after pillar failure, transferred through the roof strata. Deformation of roof strata, including immediate and main roofs, becomes more active when the mined area reaches a certain size characteristics of the stratigraphic sequences.

Massive pillar collapses or squeezes in the development sections may occur due to either a combination of wet/soft floor and section dimension (Chen and Peng, 1999; Morsy and Peng, 2001), or a combination of insufficient pillar dimension and section dimension (Artler, 1985). If the roof strata are highly competent without discontinuities, the cantilevered action of the roof strata above and beyond the gobline is responsible for the propagation of the massive pillar failure. Roof strata behave differently depending on how closely the roof strata are approaching their collapse limit. When it is close to the collapse limit, roof convergence and pillar compression occur. Conversely, when it is far from the collapse limit, roof divergence and pillar decompression occur (Zingano et al., 2005).

In the pillared section, low pillar strength due to a combination of small size and aging was attributed to a massive pillar collapse in South Africa (van der Merwe et al., 1999). He also pointed out the inadequacy of adopting a pillar design formula for the whole country, because post pillar failure investigations showed that local pillar strength were less than the nationally used value.

Zipf and Mark (1996) stated that the rate of load transfer is related to the post-failure characteristics of the pillar, which in turn depends of the width-to-height ratio of the pillar. Slender pillar with a low width-to-height ratio shed their load rapidly because after reaching their peak strength, their strength drops rapidly, and are capable of carrying little or no load (i.e., strain-softening). On the other hand, squat pillars with a high width-to-height ratio transfer their load slowly, because after reaching the peak strength, they still maintain fairly high residual strength. In fact, some even increase their strength (i.e., strain-hardening). Data collected by Chase et al.,(1994) showed that pillar failure will occur rapidly when the width-to-height ratio is less than 3 and in those with a width-to-height ratio larger than 3, pillar failure will occur slowly (Fig. 5.6.4). This conclusion is based on the local mine stiffness concept (see Section 9.3.4, p. 438) in that the post-failure stiffness of specimens with low width-to-height ratios is less than the local mine stiffness, thereby causing them to fail rapidly. The reverse is true for specimens with high width-to-height ratio. Extrapolation of in-situ coal pillar tests from Fig. 5.6.5 indicates that when the width-to-height ratio is larger than 4, the post-failure stiffness of a coal pillar becomes positive.

3. Failure Prevention

Several methods are available for prevention of massive pillar failures. For instance, one is a proper combination of panel (or section) and pillar dimensions plus barrier pillars. Another one is to design the individual pillars with proper mechanical characteristics (Zipf and Mark, 1996).

As stated earlier, a great majority of massive pillar failures occurred when the panel (or section) reached a critical dimension, which depends on the characteristics of roof strata and pillar dimensions. Consequently, for each type of immediate roof and stratigraphic sequence, a proper combination of pillar and panel dimensions is required. For this approach, numerical computer analysis is desirable.

Alternatively, when barrier pillars are used to contain massive pillar failures, panel pillars should have a width-to-height ratio greater than 4 and a safety factor of at least 2 on

development and 1 on retreat (Zipf and Mark, 1996). The barrier pillar should have a width-to-height ratio greater than 10.

Mine structural analysis has also been used to study the cause of massive pillar collapse considering local mine stiffness (Morsy and Peng, 2001 and 2002a). This approach can address more diverse conditions, including when weak floor due to water ponding is the major contributor to massive pillar failures.

Unfortunately, none of the causes identified so far consider the time factor or why some pillar collapses occur suddenly and others occur and propagate gradually.

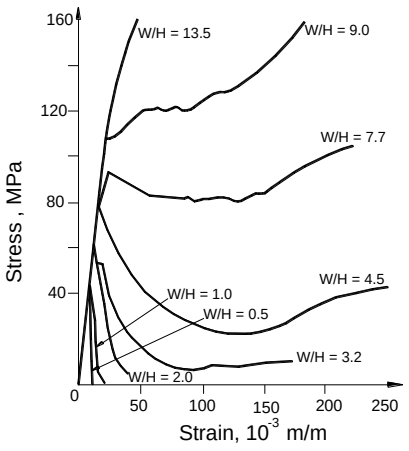

Fig. 5.6.4 Complete stress-strain curves for specimens with various W/H ratios (Das, 1986)

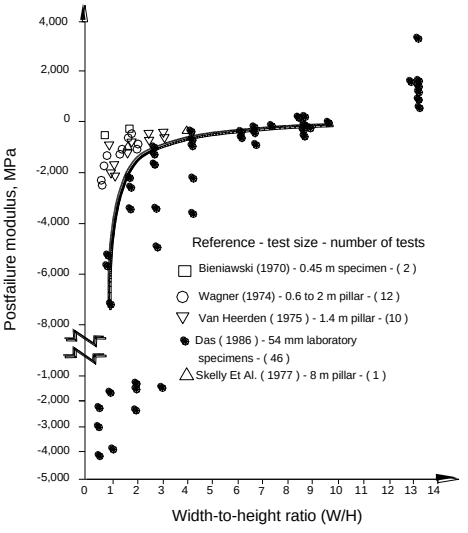

Fig. 5.6.5 Post-failure moduli of coal pillars and specimens (Chase et al., 1994)

5.6.3 Pillar Bumps

Bumps are sudden violent failures of coal pillars accompanied by audible noises and ejection of coal debris. The amount of coal debris ejected ranges from tiny chips to hundreds of tons, while the noises vary from barely audible to more than 4 on the Richter scale, which often is accompanied by air blasts.

As shown in Figs. 5.4.2 and 5.4.3, only the critical pillars are liable to bumps, and the size of critical pillars are dependent on site-specific geological conditions. This may be why the critical pillar width-to-height ratio, below which pillars are subject to bumps, varies from 3 to 8 depending on the researchers (Babcock and Bickel, 1984; Brauner, 1994; Campoli et al., 1990; DeMarco et al., 1995; Holland, 1958b; Mark et al., 2002b; and Ozbay, 1989).

For a more detailed discussion about coal bumps, refer to Chapter 9, Bumps, p. 422.

5.7 LONG-TERM VERSUS SHORT-TERM PILLAR STRENGTH

All the pillar design formulae or methods discussed so far are static or short-term pillar strength. **Short-term** may range from 1 to 5 years depending on the size of the mine. **Long-term**, however, means the mine's lifetime or more than 10 years.

It is generally an accepted practice that pillars that must last longer are bigger and those for temporary use are smaller. Therefore, pillars in the mains are larger than those in the submains, that in turn are larger than those in the sections or panels, because the length of service life, in decreasing order, is mains, then submains, and finally production panels or sections. This concept is normally implemented by adopting the largest safety factor for main pillars and the smallest for pillars in production panels or sections. This concept of pillar design also implies that the safety factor is closely related to time-dependent strength of a pillar.

The 1977 Surface Mining Control and Reclamation Act (SMCRA) (U.S. Congress, 1977b) requires that underground mining should not cause surface subsidence now and/or in the future. In implementing this statute, the questions "Will any existing underground pillars be stable permanently, and how will we design underground pillars that will remain stable in the future?" must be answered satisfactorily.

The industry rule of thumb was that if the extraction ratio in room-and-pillar mining was less than 50%, pillars would be stable permanently, because anecdotal evidence indicates that surface subsidence has never occurred under such condition.

Citing for the fact that Salamon and Munro's formula was based on the analysis of full-sized pillars that stood for some time before failing, tens of years in some areas, so the recommended safety factor of 1.6 is intended to indicate the stability of the pillar for the long term (Madden, 1992). Madden (1992) also stated that since beyond a safety factor of 2.1, the probability of stable geometry only increases marginally, so for long-term stability, pillars with a safety factor of 2.1 and width-to-height ratio greater than 4 are recommended.

Similarly, Bieniawski et al., (1994) stated that for the Bieniawski formula, the recommended safety factors of 2.0 for mains and retreat panels and 2.5 for barrier pillars are for long-term pillar stability.

Van der Merwe (1998) stated that there is no correlation between safety factor and pillar life and that the observed failure mode was severe scaling, while the roof remained more or less intact, and therefore, progressive scaling or sloughing is the cause of pillar failure. He proposed the pillar life equations for Vaal Basin, South Africa as,

$$L_{pv} = 0.025\,(L_p + 2)^{2.5} + 2.178 \tag{5.7.1}$$

$$L_p = d_v / r_{vp} \tag{5.7.2}$$

$$d_v = W - (0.074\, h^{0.268}\, H^{0.407}\, C^{0.813}) \tag{5.7.3}$$

$$r_{vp} = (r_h^5 r_i)^{0.1667} \tag{5.7.4}$$

$$r_h = 0.008\, h^4 + 0.44 \tag{5.7.5}$$

$$r_i = 16.453\, e^{-1.7 L_v} + 0.878 \tag{5.7.6}$$

where L_{vp} is actual pillar life, L_p is predicted pillar life, r_{vp} is predicted scaling rate for Vaal Basin, d_v is Vaal Basin scaling distance, W is pillar width, h is mining height, H is mining depth, C is pillar centers.

Pillar scaling is due in part to weathering. Weathering was found to be the key factor for long term pillar strength of the Pittsburgh coal (Biswas et al., 1999; Biswas and Peng, 1999). A strength profile exists in a pillar that is not only nonlinear but also varies in form and

magnitude in different layers in the pillar. The three most distinct regions in a strength profile are:

Zone 1 – lower strength at the rib side,
Zone 2 – gradual increase in strength from the rib side to the core, and
Zone 3 – intact strength in the core.

The slope of zone 2 (i.e., the rate of gradual increase in strength) is dependent on the material and the degree by which it is susceptible to weathering processes. The rocks in partings are more vulnerable to weathering processes in the presence of moisture. Strength profiles of pillars 5, 15, and 50 years old as measured by a borehole penetrometer demonstrated that weathering causes the coal and partings to deteriorate with time and that soft parting degrade much faster than coal. The measured data were used to derive the following pillar life equations for the Pittsburgh coal.

For partings $$P_p\,(\%) = 100\,(1.01 - e^{-0.5\,H}) - 0.45\,T \qquad (5.7.7)$$

For coal $$P_c\,(\%) = 100\,(1.01 - e^{-3\,H}) - 0.13\,T \qquad (5.7.8)$$

where P_p and P_c are strength for parting and coal at year T in percentage of the original intact parting and coal strengths, respectively, and H is mining depth.

5.8 PILLAR EXTRACTION

5.8.1 Mobile Roof Supports (MRS)

Traditionally, pillar extraction used a lot of wood posts as turn and breaker posts to support the gob lines, separating the continuous miner from the gob (Kauffman et al., 1981). Using wood posts as gobline supports has many disadvantages. Among them, wood posts are heavy and miners must erect them physically at the gobline, exposing them to potential of gob override, rib spalling, and back injuries. Wood posts are less stable and tend to be knocked out of position due to gob movement. In addition, wood posts are passive supports and roof coverage is small (Chase et al., 1997). Due to these adversities, pillar extraction was declining steadily in the 1980s (Montague, 1988). The introduction of mobile roof supports (MRS) (Fig. 5.8.1) in the early 1990s (Wilson, 1991) reversed the trend.

Mobile roof supports, similar in principle to shield supports for longwall mining (Maleki et al., 2001; Follington et al., 1992), is more suitable for gobline support, correcting all of the disadvantages of wood posts. MRS is of two models: one has 600-ton and the other has 800-ton capacity with working height ranges from 36 in. (0.9 m) to 162 in. (4.1 m). An MRS is stable and better suited to resist horizontals movements and forces that are common along the gobline. Also an MRS has lateral capacity (parallel to gob line direction) of 62.5 tons (556 KN) and horizontal capacity (perpendicular to gob line direction) of 87.5 tons (778 KN). Each MRS has a bearing capacity of approximately six timber posts and equivalent stiffness to two or more posts (Barczak and Gearhart, 1997).

MRSs are deployed as a set of four units. Figures 1.3.8, 1.3.10, and 1.3.11 (p. 9 – 12) show the methods of pillar extraction using MRSs. The location of MRSs is most important during retreat pillar mining. They should be moved as often as and kept as close as possible to the continuous miner to reduce the possibility of premature roof caving. This is especially true at the intersections of entries and crosscuts. A proper setting load can be determined by monitoring the roof bolt load. The bolt loads should be decreased when the MRSs are set, but

should be able to support the incremental load resulting from the release of MRSs while tramming. (Hay et al., 1995).

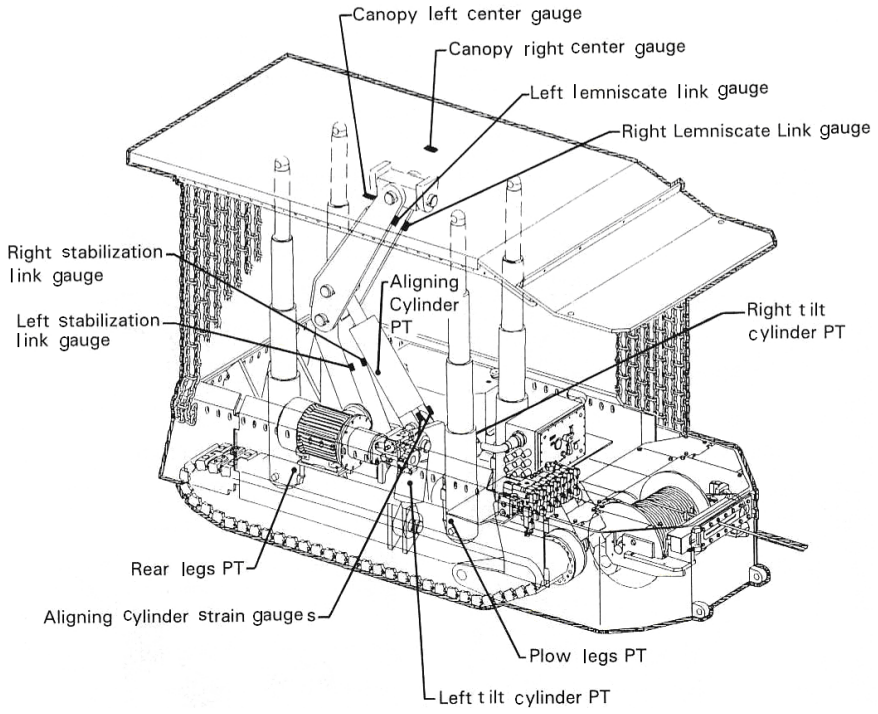

Fig. 5.8.1 Mobile Roof Support (Barczak and Gerahart, 1997)

5.8.2 Pillar Design for Pillar Extraction

Pillar dimensions for areas intended for secondary mining, i.e., pillar extractions, are different from those intended for first mining (development mining), because extraction of pillars creates gobs that, just like retreat longwall mining, induces abutment pressures around the edges of the gob. The major difference between first and secondary mining is pillar loading. In first mining, pillar load can be estimated by the tributary weight of overburden above it (i.e., development load), while in secondary mining, pillars near the gobline are subjected to the tributary overburden (development) load plus abutment loads.

There are two major pillar design methods for pillar extraction: three-dimensional numerical computer analysis (Peng et al., 2007b) and conventional pillar design formula. The advantages of numerical modeling are that it can fully account for site specific conditions, including strata caving, stump pillars, and odd geometry. Conversely, the design formula method is simple to use.

Using the same principle as ALPS (see Fig. 5.3.10, p. 251), Mark and Chase (1997) developed the analysis of retreat mining pillar stability (ARMPS) method, featuring a new pillar strength formula that considers the length effect of rectangular pillars and the introduction of an **active mining zone** (AMZ), which is the zone width of the front abutment load outby the pillar line (Fig. 5.8.2). Just like all other pillar design formulae, ARMPS consists of three steps:

1. Pillar Loading

There are four types of loadings: Loading 1 consists of development load only. Loading 2 has one active retreat section consisting of development load plus one front abutment load. Loading 3 has an active retreat section and one side gob, consisting of the development load plus one front abutment load plus one side abutment load. Loading 4 has an active retreat section and one gob on each side of the section, consisting of the development load plus one front abutment load plus two side abutments. The width of the active mined zone (AMZ) is determined by

$$AMZ = 5\sqrt{h} \tag{5.8.1}$$

where h is depth of cover.

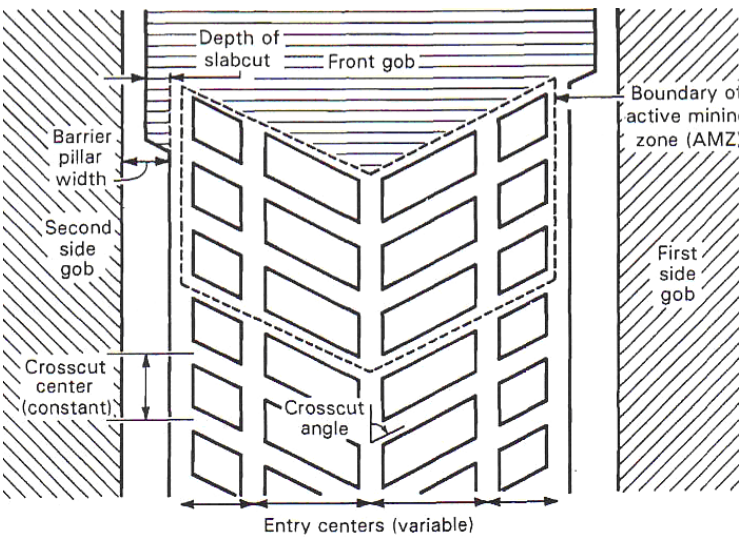

Fig. 5.8.2 Parameters used in ARMPS (Mark and Chase, 1997)

2. Pillar Load-Bearing Capacity

The pillar strength considering the effect of pillar length is represented by Equation 5.3.27

$$S_p = S_c\left\{0.64 + \left[0.54\frac{W}{H} - \left(0.18\frac{W^2}{LH}\right)\right]\right\} \tag{5.8.2}$$

where S_c = 900 psi (6.2 MPa) is in-situ coal strength, W is pillar width, L is pillar length, and H is pillar height.

The load bearing capacity of the pillars is equal to pillar strength multiplied by their load bearing area,

$$L_p = S_p\left[(W_0 + L)(W_0 + W) - W_0(W_0 + L) - \frac{W_0(W_0 + W)}{\sin\phi} + \frac{W_0^2}{\sin\phi}\right] \tag{5.8.3}$$

where W_o is width of entry and crosscut, W is pillar width (rib to rib), L is pillar length (rib to rib) and ϕ is angle between the crosscut and the entry.

3. Safety (Stability) Factor

ARMPS is calibrated using case histories of successful and unsuccessful designs. The recommended safety factors vary with depth of cover as shown in Fig. 5.8.3. For cover less than 650 ft (198 m), the recommended safety factor is 1.5. For cover from 650 to 1,250 ft (198 to 381 m) deep, the recommended safety factor decreases from 1.5 to 0.9. For cover greater than 1,250 ft (381 m) deep, the recommended safety factor is 0.9. Note that for cover greater than 750 ft (228.6 m), there were more successful cases than unsuccessful ones with safety factors lower than the recommended values.

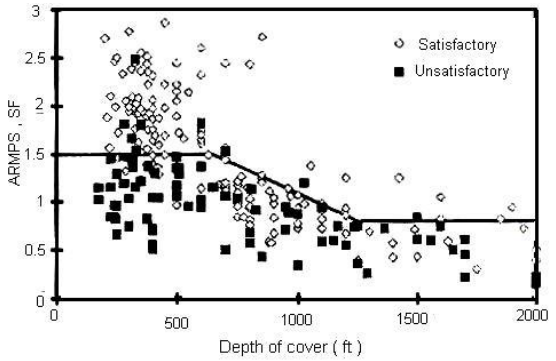

Fig. 5.8.3 The ARMPS case history data base and recommended safety factors showing the effects of increasing depth of cover (Chase et al., 2002; Mark et al., 2002b)

The recommended safety factors for ARMPS have been revised several times since its introduction in 1997 (Chase et al., 2002). In 1999, Mark (1999) recommended SF = 2.00 - 0.016 CMRR. The latest recommendations include a minimum safety factor equal to or greater than 1.5 at depths below 650 ft (198 m). At depths greater than 650 ft (198 m), the recommended safety factors vary as shown in Table 5.8.1 (MSHA, 2008). ARMPS also recommends that when depth is greater than 1,000 ft (304.8 m), barrier pillars should be used and the pillar safety factor should be considered in conjunction with that of barrier pillars. Minimum recommended barrier pillar safety factors are 1.5 for strong roof and non-bump-prone ground and 2.0 for weak, intermediate and strong roof in bump-prone conditions. Just like any other empirical formulae derived purely from case studies, ARMPS is only applicable to the mining and geological conditions covered by the case studies. For this reasons, MSHA (2008) has issued precautions for the use of ARMPS.

ARMPS is not just for retreat mining. It can be used for development, in which case, it simply uses the Mark-Bieniawski formula with the tributary area loading, precisely as discussed with other conventional pillar strength formulae described in Section 5.3.1 (p. 238).

Table 5.8.1 Recommended safety factors for ARMPS (MSHA, 2008)

Depth, H	Weak and intermediate roof strength	Strong roof
650 ft ≤ H ≤1,250 ft	1.5 – [(H - 650) /1000]	1.4 – [(H - 650) /1000]
1.250 ft ≤ H ≤ 2,000 ft	0.9	0.8
Barrier pillar SF		
H > 1,000 ft	≥2.0	≥1.5
		≥2.0

5.9 WEB PILLAR FOR HIGHWALL MINING

The concept of highwall mining has its origin from auger mining, which was rather popular in the 1940s-1960s. Circular holes are augered from the highwall into the coal seam to 100-200 ft (30.5-61 m) deep. Due to its circular shape, the pillar between adjacent holes assumes an hour-glass shape and is more stable than a rectangular one. However, the short penetration depth sterilized considerable reserve, so the highwall miner was introduced in the early 1980s. In addition to new thin-seam reserves, it can also re-mine those abandoned reserves previously mined by augers (Amick, 2007; Newman and Zipf, 2005; Zipf, 2005a). But its application did not receive due attention until the mid 1990s. In the meantime, penetration depth in auger mining continues to increase.

Highwall mining, just like auger mining, is intended for thin seam coals, although some models can mine up to 6 ft (1.8 m) thick. It can reach up to 1,500 ft (467.3 m) deep with a remote guidance system.

Highwall mining involves two types of ground control issues: pillar design and highwall stability. Highwall stability is discussed in Chapter 14 (p. 664). There are two types of pillars used in highwall mining: web and barrier pillars (see Fig. 1.3.19). A **web pillar** is the pillar left between two adjacent cuts of the highwall miner for the purpose of supporting the overburden. A **barrier pillar** separates the effects of mining one panel from the adjacent panel (Fig. 5.9.1). In recent years, the most common statistics for highwall mining in the U.S. were (Zipf and Bhatt, 2004; Zipf and Mark, 2005)

Mining depth: 82 % less than 300 ft (91 m), maximum 500 ft (152 m).
Seam thickness: 75 % 3 – 6 ft (0.9 – 1.8 m), maximum 7 ft (2.1 m).
Web pillar:
- Width: 3 – 7 ft (0.9 – 2.1 m).
- Width/height 50 % at 10-1.25, 25 % each at 0.5 -1.0 and greater than 1.25
- Length up to 1,500 ft (467.3 m)

Barrier Pillar 10 – 25 ft (3 – 7.6 m)
Panel size (i.e., number of holes between adjacent barrier pillars):
- Hole size (i.e., width of cut)
  - 9 – 12 ft (2.7 – 3.6 m), depending on the type of continuous miner used. 37% with no more than 20 holes, 44 % with 10 holes, 15 % with 5-10 holes.

Due to their long length and narrow width, it is critical that the width of web and barrier pillars be maintained all throughout their lengths. For example, an orientation alignment error of a mere 6 in. in an 800-ft (243.8 m) long cut results in a 1-ft (0.3 m) deviation in web pillar width, which ranges from 14 to 33 % of the 3-7 ft web pillar width used. And since the pillar length may reach up to 1,500 ft (467.3 m), seam, roof, and floor conditions are most likely not uniform and, therefore, a three-dimensional structure is created. Under such condition, panel dimensions, i.e., both the panel width and length must be considered for more accurate pillar system design. In a three-dimensional structural design, the following design parameters are considered: width and length of web and barrier pillars in a panel, number of holes in a panel, and number of consecutive panels along highwall.

According to Zipf (1999), two methods are available for highwall web pillar design, the conventional strength-based and the post-failure analysis. In the conventional strength method, the applied stresses are always less than the strength of a structure. In the post-failure design method, pillar size is determined based on the strength and failure characteristics. Therefore in

this method, the desired failure characteristics of the pillars are selected first, from which pillar width, number of pillars and panel width are then determined.

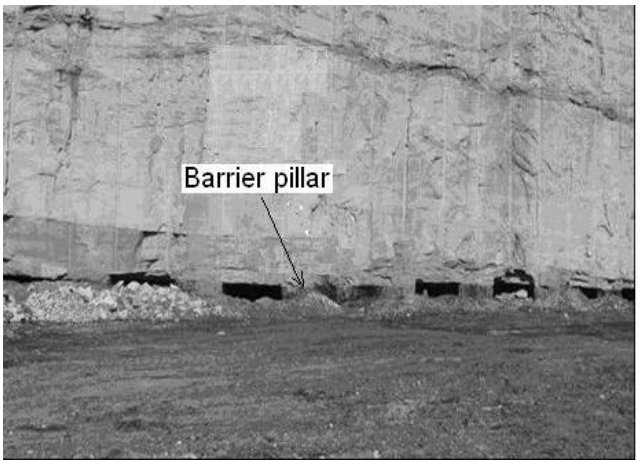

Figure 5.9.1 Typical highwall miner holes and web pillars. Note that barrier pillar or "skip hole" indicated by arrow (Zipf, 2004)

Zipf (2005a) developed design charts for web and barrier pillars: (1) assuming pillar loading by the tributary loading, and (2) using the Mark-Bieniawski formula (see Equation 5.3.27) with default pillar strength of 900 psi (6.2 MPa).

The stability factor for a web pillar (Newman and Zipf, 2005) is

$$SF_{web} = \frac{S_{cube}\left\{0.64 + \left[0.54\frac{W}{H} - 0.18\left(\frac{W_p^2}{HL}\right)\right]\right\}}{\frac{\sigma_v\left(W_p + W_o\right)}{W_p}} \tag{5.9.1}$$

where SF_{web} is the safety factor for web pillar, S_{cube} is in-situ coal strength, σ_v is in-situ vertical stress, W_p is web pillar width, W_o is cut width of highwall miner, L is web pillar length, and H is mining height.

For highwall mining, the pillar length is much longer than the pillar width and height, so the last term of the Mark-Bieniawski formula can be ignored. Equation 5.9.1 thus becomes,

$$SF_{web} = \frac{S_{cube}\left(0.64 + 0.54\frac{W_p}{H}\right)}{\frac{\sigma_v\left(W_p + W_o\right)}{W_p}} \tag{5.9.2}$$

The recommended safety factor for web pillars is 1.5.

The panel width, W_{pn}, between barriers is

$$W_{pn} = N\,(W_p + W_o) + W_o \tag{5.9.3}$$

where N is number of web pillars in a panel.

The stability factor for the barrier pillar (Newman and Zipf, 2005) is

$$SF_{bp} = \frac{S_{cube}\left(0.64 + 0.54\frac{W_{bp}}{H}\right)}{\frac{\sigma_v\left(W_{pn} + W_{bp}\right)}{W_{bp}}} \tag{5.9.4}$$

where SF_{bp} is the safety factor for barrier pillar, and W_{bp} is the barrier pillar width. Since Equation 5.9.4 neglects the stress carried by the web pillars, the stability factor for the barrier pillars can be as low as 1.0. However, the recommended width-to-height ratio for the barrier pillars is greater than 3.

ARMPS-HWM program can be used to calculate the stability factors for both the web pillars and barrier pillars (Mark, 2006).

Figures 5.9.1 and 5.9.2 show examples of the design charts for web and barrier pillars, respectively

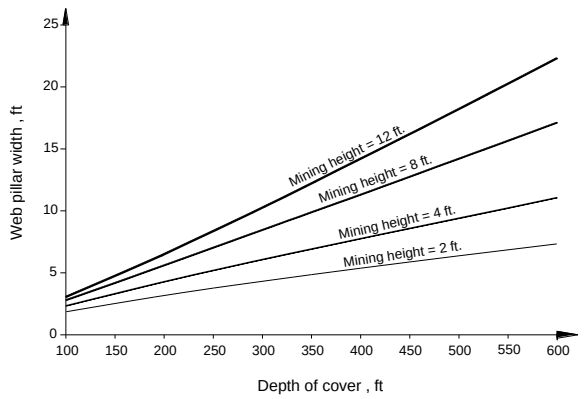

Fig. 5.9.1 Suggested web pillar width with stability factor of 1.6, and 9 ft (0.9 m) wide hole (Newman and Zipf, 2005)

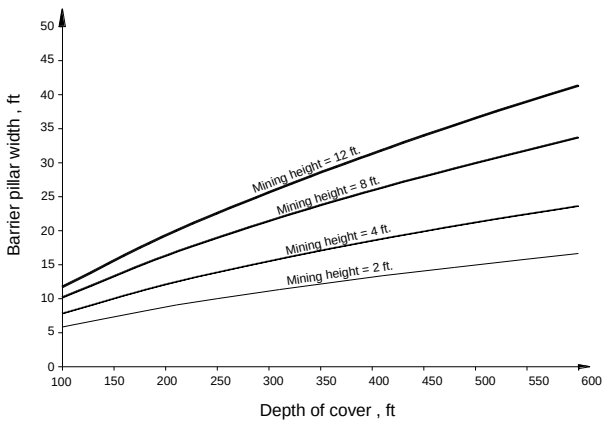

Fig. 5.9.2 Suggested barrier pillar width for 100 ft (30.5 m) wide panel with stability factor of 1.0 (Newman and Zipf, 2005)

5.10 DEWATERING AND PILLAR STRENGTH

In the past two decades, surface subsidence resulting from underground mining and its damage to residences have been attributed to dewatering of abandoned or flooded mines.

When abandoned mines are flooded with water, the confining pressure offered by the water head will reach a new equilibrium with the submerged coal pillars. Later, when the decision is made to re-mine these abandoned areas, the water must be pumped out. Will dewatering de-stabilize the pillars and induce surface subsidence and subsidence damage? Case histories showed conflicting results.

In Indiana, a surface mine was stripping and pumping water from the #7 coal seam, which was overlying the #6 coal 55 ft (16.8 m) below. The #6 coal was extensively mined with room-and-pillar mining 40-50 years previously. The abandoned #6 coal mines were completely flooded, and in fact, its water head had risen beyond the #7 coal, which then required dewatering prior to stripping. Residents above the abandoned mines claimed dewatering in the #7 coal, which was hydrologically connected to #6 coal, weakened the remnant pillars in the abandoned #6 coal mines, causing subsidence damage to their houses (Chandrashekhar and Peng, 1994). Surface subsidence was monitored over a period of two years while pumping was continued in the #7 coal. There was no evidence of surface subsidence even when the water head was dropped down 30 ft (9.1 m) in a period of two weeks.

When an active mine in the Upper Freeport seam accidentally broke into abandoned workings full of water due to an inaccurate old mine map, the active workings were flooded with a water head of 75 ft (22.9 m). It took mine management 6 months to pump out the flooded water (Peng, 2007). After the flooded mine was pumped dry, the pillar ribs remained intact, showing no sign of change before and after flooding, even though roof falls (mainly skin falls) occurred extensively (Fig.5. 10.1).

Fig. 5.10.1 Flooding caused the immediate roof to peel off between bolts, while the pillar remained intact. A large roof fall occurred in the background (Peng, 2007)

A longwall set-up room including 5 pillars outby the headgate and tailgate was flooded to a depth of 26.2 ft (8 m) above the roofline for 10 weeks (Payne, 2008). A wave action existed at the water edge. After pumping dry, the ribline was in excellent condition. Where there was clay in the seam or above the seam the wave action would wash it out slightly and in some places created a gap over the pillar at the roof line but did not cause any problems.

Kohli (1992) reported a surface subsidence case involving abandoned workings in two coal seams. The upper seam, 250-280 ft (6.2-85.4 m) deep, was mined 11 years prior to the lower seam 400 ft (122 m) below. Both seams were mined by room-and-pillar mining without pillar extraction. After several years of mining, the lower seam was flooded due to unfavorable market conditions. Later, when management decided to re-enter the lower seam, water was pumped out and subsidence cracks soon appeared on the surface. In an effort to determine the cause, surface boreholes were drilled and rock cores were recovered. Fresh cracks were found in the overburden strata between the upper and lower seams. It was determined that dewatering most likely weakened the pillars disrupting the overburden.

5.11 PILLAR DESIGN FOR GAS/OIL WELLS

In eastern and central coalfields, there are many gas wells, both active and abandoned, drilled through coal seams that are being actively mined. There are two ways to deal with those wells. One is to plug them, and the other is to design the panel layout in such a way that gas wells are located in the chain pillar system between the panels. The former method is very expensive, whereas the latter, when feasible, is more effective. If there are many gas/oil wells in close proximity, pillar sizing becomes a critical issue because, invariably, the location of one or more gas/oil wells would not satisfy the existing pillar plan required by law.

In placing a gas well in the chain pillar system, several factors must be considered in order to assure its integrity after longwall mining. Because longwall mining not only causes surface and subsurface subsidence within and beyond the panel edges, it also induces high abutment pressures around the edges of the panel. The effect of longwall mining on a gas well is determined by considering the overburden depth, abutment pressure, pillar size, and the location of the gas well with respect to the panel edge. A properly designed pillar (or pillar system) should protect the gas well located within it from longwall mining effects.

In the state of Pennsylvania (1957), the adopted pillar plans call for different pillar bearing areas for various depths of mining (Fig.5.11.1).

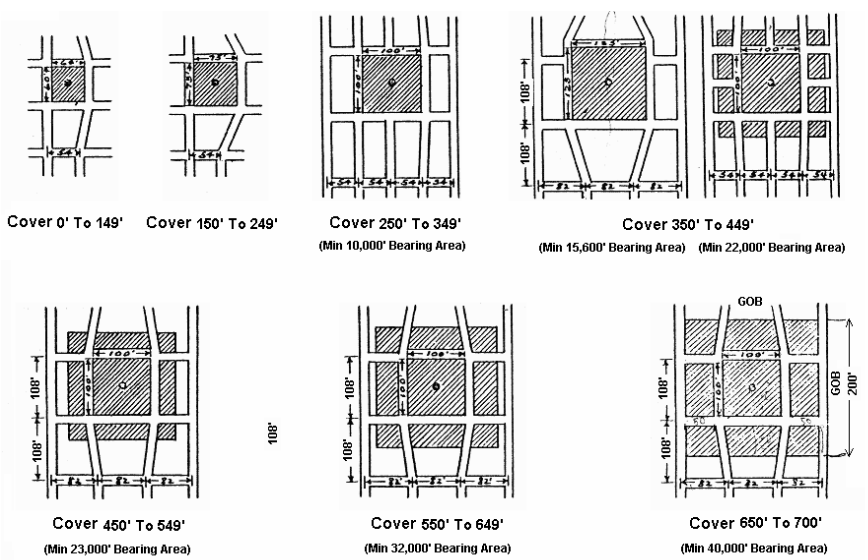

Fig. 5.11.1 State of Pennsylvania pillar plan for protection of gas/oil wells (State of Pennsylvania, 1957)

The bearing area consists of a solid core pillar plus additional pillars surrounding it. The pillar core starts from 60 ft (18.3 m) square for depths below 150 ft (45.7 m) to a maximum of 100 ft (30.5 m) square for depths above 250 ft (76.2 m). The additional pillars surrounding the core also increase with the depth until it reaches a maximum total pillar dimension of 200 ft (70 m) square, with the gas well at the pillar center when the mining depth is 650 ft (198.2 m) or more. In recent years, as long as the total pillar bearing areas meet the size requirement, the location of a gas well in the core pillar is allowed to be off-center if the minimum distance from the gas well to the panel edge is 50 ft (15.2 m) or more (Fig. 5.11.2).

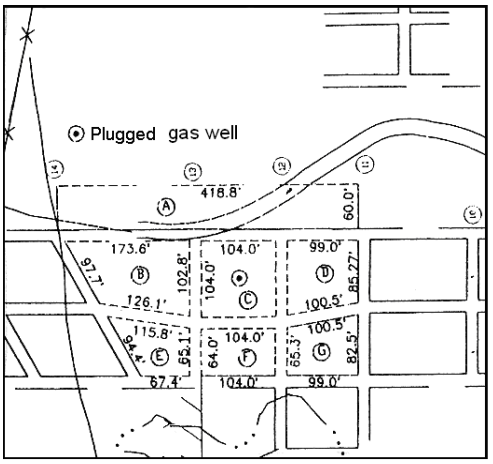

Fig. 5.11.2 Alternate pillar plan for gas well protection

Pillar research in the past few decades has shown that this supporting plan is over-conservative in many cases. What then is the appropriate pillar size, and is the pillar the only factor in gas well protection in longwall mining? The best approach is to perform three-dimensional mine structural analysis for optimum location of gas/oil wells and pillar configuration. For instance, based on 3-D FE modeling, Peng et al., (2003) analyzed the cause for gas well casing failure and successfully determined that it was caused mainly by vertical deformation (or vertical subsidence), and to a lesser extent by horizontal deformation (or horizontal displacement), at the seam level and near the seam in the roof or floor. The gas well casing was forced to move with the surrounding rock of the borehole as a unit after, but not before, the next adjacent panel was mined. The location of gas well failure was in the soft strata at and near the coal seam being mined. The softer the strata, the larger the deformation, and the more likely the location where the gas well casing will fail.

5.12 CASE EXAMPLES-PILLAR DIMENSIONS USING VARIOUS DESIGN METHODS

With so many pillar design formulae/methods available, two things must be kept in mind in the design of various types of coal pillars. For one thing, any formula will not be applicable for all geological and mining conditions (Hirt and Shakoor, 1992). In fact, there are many stories of pillar failures or not being functionally successful when using certain formula for the whole district or mine. The other important factor is that local, site specific experience of pillar application must be considered, because the mining and geological conditions from which the design formulae are derived may not be applicable to the specific sites of interest.

In this section two examples are given, one in room-and-pillar mining and the other in longwall mining. In the examples, basic data, i.e., rock mechanics properties, are the same, and various pillar strength formulae and numerical methods are used to determine pillar size. Finally, the actual pillar dimensions practiced in the mine are compared.

1. Longwall Case

The mining and geological conditions for the longwall mine case are described in Section 12.6 (p. 575). The panel is 1,450 ft (442.1 m) wide and 1,000 ft (304.5 m) deep and developed by a three-entry system (see Fig. 12.6.1 on p. 577). The gateroad chain pillars adopted by mine management were diamond-shaped 110 ft (33.5 m) wide by 175 ft (53.4 m) long center-to-center. The entries and crosscuts were 16 ft (4.9 m) wide and 8.2 ft high.

For the Pittsburgh seam, the recommended safety factor for ALPS is 1.2 (1.76 – 0.014 CMRR) with an average CMRR of 40. For SF of 1.2, ALPS recommends pillar size be 94.4 ft (28.8 m) wide by 159 ft (48.5 m) long. The pillar size adopted by mine management is the same as recommended by ALPS.

The pillar design equation proposed by Hsiung and Peng (1985a) is

$$\log(W_P) = \left\{-0.008134\frac{E_i}{E_c}\right\} - \left\{0.004133\frac{E_m}{E_c}\right\} + \left\{0.0136\frac{H_m}{H_c}\right\} - \left\{0.172\log\left(\sigma_m\right)\right\} + \left\{0.751\log\left(h\right)\right\} + \left\{0.039\log\left(d\right)\right\} \quad (5.12.1)$$

where W_p is pillar size, σ_m is minimum uniaxial compressive strength of coal, h is depth of cover,, d distance between the set-up room and face, E_m is the Young's modulus of the main roof, E_i is the Young's modulus of the immediate roof, E_c is the Young's modulus of coal, H_m is thickness of the main roof, and H_c is mining height. Substituting the rock properties values from Table 12.6.2 (p. 578) into Equation 5.12.1, the recommended square pillar size is 81 ft (24.7 m).

Using the Wilson formula (Wilson and Ashwin, 1972), the recommended pillar size is 25 x 161 ft (7.6 x 49 m).

Numerical modeling using FLAC^{3D} shows that the 110 ft (33.5 m) wide by 175 ft (53.4 m) long centers pillars will have no problems during panel 1 (retreat 1) mining (see Fig. 12.6.7 on p. 584 and Fig. 12.6.13 on p. 589). During panel 2 (retreat 3) mining, however, the tailgates will require supplementary supports.

2. Room and Pillar Case

The mining and geological conditions for the room and pillar mine case are described in Section 12.5 (p.563). Table 5.12.1 shows the barrier and chain pillar sizes recommended by various pillar design formulae and methods.

To estimate the mains barrier pillar width, in ARMPS the loading conditions was selected as active retreat section and two side gobs. The extent of active gob was taken as 450 ft while the extents of gob in both sides of the active panel were 650 ft. The default value of abutment angle, 21o was used. In the retreat part of input information, an arbitrary barrier pillar width was assumed and corresponding stability factors were checked from the output. The barrier pillar width for which the stability factor exceeds 2.0 was finally selected as the required mains barrier pillar width. The same steps were followed for estimation of inter-panel barrier width but with the loading condition as active retreat section and one side gob. Similar procedure was followed for mains and panel pillar estimation. For numerical modeling methodology and results, refer to Section 12.5 for detail. Note that in numerical modeling, the chain pillars 50 x

50 ft (15.1 x 15.2 m) were chosen by mine management based on their experience for maximum production effectiveness. Numerical modeling in this case was to confirm that the pillar size would perform satisfactorily during various stages of mining.

Table 5.12.1 Pillar dimensions determined by various pillar design formulae

Type of Pillar		Bieniawaski[1] (Mark-Bieniawaski)[2]	ARMPS[3]	Numerical modeling (FLAC)[4]	Peng's formula[5]	Mine inspector barrier formula[6]	British barrier formula[7]
Barrier pillar, ft	Mains		50	260	225	92.6	103.6
	Inter-panel		50	140			
Chain pillar, ft	Mains pillar	30 x 30 (32 x 32)	40 x 40	50 x 50			
	panel pillars		40 x 40	50 x 50			

[1] See Equation 5.3.12 on p. 240
[2] See Equation 5.8.2 on p. 277
[3] See Section 5.8.2 on p. 276
[4] See Section 12.5 on p. 563
[5] See Equation 7.4.1 on p. 340
[6] See Equation 5.5.1 on p. 260
[7] See Equation 5.5.3 on p. 268